

# Covert Signaling for Communication and Sensing over the Bosonic Channels

Tianrui Tan<sup>1</sup>, Evan J. D. Anderson<sup>2</sup>, Michael S. Bullock<sup>3</sup>, and Boulat A. Bash<sup>1</sup>

**Abstract**—Preventing signal detection in communication and active sensing requires careful control of transmission power. In fact, the square-root laws (SRL) for covert classical and quantum communication and sensing prescribe that the average output power per channel use scales as  $1/\sqrt{n}$  for  $n$  channel uses. Two strategies for achieving this are *diffuse* and *sparse* signaling. The former transmits signals with power decaying as  $1/\sqrt{n}$  on all  $n$  channel uses, which is convenient for mathematical analysis. The latter transmits constant-power signals rarely, on approximately  $\sqrt{n}$  out of  $n$  channel uses, while remaining silent on the others. This offers significant practical advantages in compatibility with modern digital transmitters. Here, we study sparse signaling over lossy thermal-noise bosonic channels, which describe quantumly many practical channels (including optical, microwave, and radio-frequency). We characterize the input signal state that minimizes detectability. We find an unintuitive optimal quantum state structure: a mixture of just two consecutive photon-number states. In particular, in the low-brightness regime, the optimal signal state is a mixture of vacuum and a single photon. Since these states are generally suboptimal for both communication and active sensing, we explore the resulting trade-off and identify input-power thresholds for transitions between optimizing for covertness vs. performance in communication and sensing tasks.

a non-vanishing  $\sqrt{n}$ -scale amount of information can still be sent. The square-root law and its refinements have since been developed for additive white Gaussian noise channels, discrete memoryless channels, classical-quantum channels, and networked covert communication settings [3]–[6].

For optical, microwave, and radio-frequency (RF) systems, the lossy thermal-noise bosonic channel provides the natural quantum-mechanical model of propagation loss and background noise. Each channel use corresponds to an electromagnetic-field mode, Alice’s inputs are quantum states of this mode, and Willie may in principle perform arbitrary quantum measurements on his received systems. Thus, even when coherent-state modulation and coherent detection reduce the problem to a classical Gaussian model, the ultimate covert limits require a quantum information-theoretic treatment. Prior work established the square-root law for quantum-secure covert communication over bosonic channels and characterized covert communication constants and capacities under classical-secret and entanglement-assisted resources [5], [7], [8]. These results show that thermal noise inaccessible to Willie is the resource that enables covert communication against a quantum-powerful warden.

Covert active sensing imposes a closely related Willie-side constraint. Instead of transmitting a message to Bob, Alice probes a target region and tries to discriminate between target absence and target presence while remaining undetected. This setting is motivated by quantum illumination, where signal-idler correlations can improve target detection in noisy and lossy regimes. In the covert setting, Alice’s probing signal must also be hidden from Willie. Previous work studied signaling strategies for covert quantum sensing over lossy noisy bosonic channels and compared diffuse signaling, which spreads a small number of photons over many modes, with sparse signaling, which transmits actively in only a small fraction of modes [9]. The common feature in both covert communication and covert sensing is that Alice’s operational goal is limited by the distinguishability of Willie’s state from the innocent thermal state.

The characterization of signaling schemes are central to this paper. Diffuse signaling is asymptotically natural: Alice uses nearly all modes but with vanishingly small energy in each mode. Sparse signaling instead keeps most modes silent and transmits only with a small activity probability. Although diffuse signaling is mathematically convenient, sparse signaling is practically important. In realistic radio-frequency implementations, finite converter resolutions, synchronization constraints, pulse-shaping requirements, and nonzero amplitude floors can prevent Alice from making every transmitted symbol arbitrarily weak. Recent software-defined-radio experiments therefore

## I. INTRODUCTION

Covert, or low-probability-of-detection/intercept (LPD/LPI), signaling addresses a security requirement that is distinct from encryption and secrecy: Alice must hide the existence of her transmission, not merely protect the information carried by it. An adversarial warden Willie observes the physical channel and attempts to decide whether Alice is silent or active. Alice must therefore communicate, or probe a target region, while keeping Willie’s received quantum state nearly indistinguishable from the state produced when Alice does not transmit.

A fundamental feature of covert communication is the square-root law. Over  $n$  channel uses, and in the absence of additional uncertainty at Willie, Alice can transmit only  $O(\sqrt{n})$  bits reliably while remaining covert; attempting to transmit more either makes the transmission detectable or prevents reliable decoding at Bob [1], [2]. Equivalently, the asymptotic rate in bits per channel use is zero, even though

<sup>1</sup>Tianrui Tan is with Dept. of Electrical and Computer Engineering, University of Arizona, Tucson, AZ, USA (email: tantianrui@arizona.edu)

<sup>2</sup>Evan Anderson is with the Wyant College of Optical Sciences, University of Arizona Tucson, AZ, USA (email: ejdanderson@arizona.edu)

<sup>3</sup>Michael S. Bullock is with the Manning College of Information and Computer Sciences, University of Massachusetts, Amherst, MA, USA (email: mbullock@umass.edu)

Boulat Bash is with Dept. of Electrical and Computer Engineering, and the Wyant College of Optical Sciences, University of Arizona, Tucson, AZ, USA (email: boulat@arizona.edu)

motivate sparse signaling as a physically relevant route to covert communication [10].

This paper asks the following structural question: under sparse signaling over a lossy thermal-noise bosonic channel, which active input state minimizes the covertness criteria under a mean photon number constraint? Existing covert-capacity results identify the  $\sqrt{n}$ -scaling and, for communication, characterize optimal throughput constants for particular resources and coding models. Existing covert-sensing work compares diffuse and sparse probing strategies. In contrast, our focus is the state-optimization problem inside sparse signaling itself: for a fixed per-mode brightness  $\bar{n}_S$ , how should the active state distribute its photon number so that Willie sees the smallest perturbation away from the innocent thermal state?

Our main contribution is a structural characterization of the sparse-signaling state that minimizes Willie's leading quantum relative entropy (QRE) coefficient. First, we show that the minimizer may be chosen Fock-diagonal. This reduces the optimization over quantum states to an optimization over photon-number distributions. Second, we derive the corresponding Willie-side QRE coefficient explicitly and express it using an orthogonal representation. This representation exposes the dependence of Willie's detectability on the factorial moments of the input photon-number distribution. Finally, using a convexity argument, we show that an optimizer is supported on at most two consecutive Fock states. In the low-brightness regime relevant to covert operations this reduces to a vacuum single-photon mixture.

We then relate this optimal sparse structure to covert communication and covert sensing performance. For communication, the low-brightness optimizer attains the Willie-side quadratic coefficient appearing in the bosonic covert-communication converse [7]. For sensing, the same optimizer matches the leading Willie-side quadratic coefficient of the diffuse scheme under matched transmitted mean photon number [9].

The rest of the paper is organized as follows. Section II introduces the bosonic channel model, the communication and sensing settings, the covertness criterion, and the sparse-signaling model. Section III proves the optimal sparse input structure. Section IV specializes the result to the low-brightness covert regime and connects it to known covert communication and sensing results. Section V compares the resulting communication and sensing performance under the same Willie-side covertness constraint. Section VI concludes the paper.

## II. PRELIMINARIES

### A. System Model

We first review the necessary bosonic systems and quantum optics background, deferring the details to a survey [11] and textbooks [12]–[15]. In our analysis of covert signaling we employ a lossy thermal-noise bosonic channel modeled by a beam splitter with environment mean photon number  $\bar{n}_B$  and transmittance  $\eta$  denoted by  $\mathcal{E}_{A \rightarrow BC}^{\eta, \bar{n}_B}$ . Fig. 1 depicts it. An electromagnetic-field mode at the transmitter's center frequency is the fundamental unit of information transmission

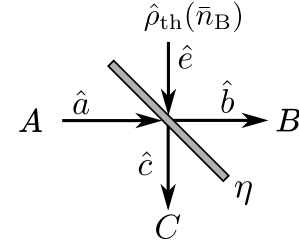


Fig. 1: The lossy thermal-noise bosonic channel  $\mathcal{E}_{A \rightarrow BC}^{\eta, \bar{n}_B}$  is characterized by transmissivity  $\eta$  and thermal photon number  $\bar{n}_B$ , with input subsystem  $A$  and output subsystems  $B$  and  $C$ . Environment is in a thermal state  $\hat{\rho}_{\text{th}}(\bar{n}_B)$ . The modal annihilation operators  $\hat{a}$ ,  $\hat{b}$ ,  $\hat{c}$  and  $\hat{e}$  are used to describe the input-output relationships in this channel.

in our work, akin to a channel use in classical information theory. System  $A$  describes the input mode, while system  $E$  is the input from the environment in a thermal state  $\hat{\rho}_{\text{th}}(\bar{n}_B)$ . Systems  $B$  and  $C$  describe the outputs. These are related to the inputs using the bosonic modal annihilation operators  $\hat{a}$  (input),  $\hat{e}$  (environment),  $\hat{b}$ , and  $\hat{c}$  (outputs). For a beamsplitter these are  $\hat{b} = \sqrt{\eta}\hat{a} + \sqrt{1-\eta}\hat{e}$  and  $\hat{c} = \sqrt{1-\eta}\hat{a} - \sqrt{\eta}\hat{e}$ . One of the output modes corresponds to the intended receiver while the other to loss of signal to the environment and/or the adversary. This describes quantum mechanically many practical channels, including optical, microwave, and radio-frequency (RF) [11].

For a single bosonic mode, the Fock state (or photon-number state)  $|i\rangle$  describes the state containing exactly  $i$  photons. Equivalently,  $|i\rangle$  is an eigenbasis of the photon-number operator  $\hat{N} = \hat{a}^\dagger \hat{a}$ , satisfying  $\hat{N}|i\rangle = i|i\rangle$ , where  $\hat{a}$  and  $\hat{a}^\dagger$  are the annihilation and creation operators, respectively. Set  $\{|i\rangle\}_{i \geq 0}$  forms an orthonormal basis for the Hilbert space of the single bosonic mode, with  $\sum_{i=0}^{\infty} |i\rangle \langle i| = \mathbb{I}$  [11]–[15]. Any quantum state of a bosonic mode can therefore be represented in the Fock basis:  $\hat{\rho} = \sum_{i, i' = 0}^{\infty} \rho_{ii'} |i\rangle \langle i'|$ , where the diagonal elements  $\rho_{ii}$  specify the photon-number distribution, and the off-diagonal elements  $\rho_{i, i' \neq i}$  encode phase relations. For example, the thermal state with mean photon number  $\bar{n}_B$  describing the environment of a bosonic channel  $\mathcal{E}_{A \rightarrow BC}^{\eta, \bar{n}_B}$  is  $\hat{\rho}_{\text{th}}(\bar{n}_B) = \sum_{i=0}^{\infty} \lambda_i |i\rangle \langle i|$ , with  $\lambda_i = \frac{(\bar{n}_B)^i}{(1+\bar{n}_B)^{i+1}}$ . Note that  $\hat{\rho}_{\text{th}}(0) = |0\rangle \langle 0|$  is a vacuum state [11]–[15].

As in our earlier works [5], [8], [16]–[18], our system employs  $n = 2TW$  orthogonal modes, which is the product of time  $T$  available for transmission, bandwidth  $W$  around the transmitter's center frequency, and the factor two corresponding to the use of both orthogonal polarizations. Thus, we consider covert communication and active sensing settings where Alice's transmission is an  $n$ -mode quantum state  $\hat{\rho}_A^n$ .

1) *Communication Model:* We model communication by a single thermal-loss bosonic channel  $\mathcal{E}_{A \rightarrow BW}^{\eta, \bar{n}_B}$  depicted in Fig. 2a. Denote the Alice-to-Bob message set by  $\mathcal{M}$  and suppose that each message  $m \in \mathcal{M}$  is equiprobable. Alice encodes  $m$  in an  $n$ -mode state  $\hat{\rho}_A^n(m)$  and transmits it to Bob via  $n$  independent uses of  $\mathcal{E}_{A \rightarrow BW}^{\eta, \bar{n}_B}$ . Bob receives the  $n$ -mode output state  $\hat{\rho}_B^n(m) = \text{tr}_W \left[ (\mathcal{E}_{A \rightarrow BW}^{\eta, \bar{n}_B})^{\otimes n} (\hat{\rho}_A^n(m)) \right]$ , and attempts to decode using a positive operator-valued measure

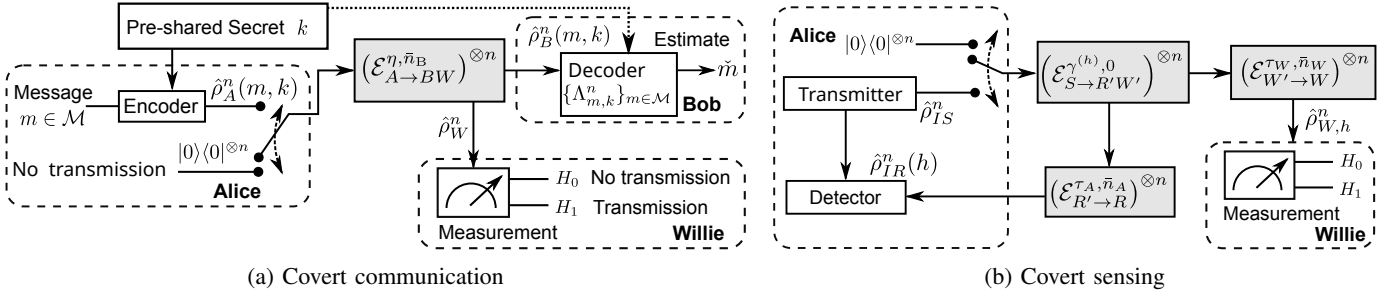


Fig. 2: Systems models for covert communication and sensing. In both models, adversary Willie has to decide whether Alice transmits based on his observed state. When she does not transmit he receives thermal state.

(POVM)  $\{\Lambda_m^n\}_{m \in \mathcal{M}}$ ,  $\sum_{m \in \mathcal{M}} \Lambda_m^n = \mathbb{I}_B^{\otimes n}$ , to produce an estimate  $\tilde{m}$  of the transmitted message. Accordingly, Bob's decoding task is to infer  $m$  from  $\hat{\rho}_B^n(m)$  with vanishing error probability [8]. Formally, the average decoding error probability is  $P_e^{(b)} = \frac{1}{|\mathcal{M}|} \sum_{m \in \mathcal{M}} \Pr\{\tilde{M} \neq m | M = m\} = \frac{1}{|\mathcal{M}|} \sum_{m \in \mathcal{M}} (\text{tr}[(\mathbb{I} - \Lambda_m) \hat{\rho}_B^n(m)])$ , where  $M$  and  $\tilde{M}$  are the random variables describing the transmitted message  $m$  and its estimate  $\tilde{m}$ . Reliability requires that  $P_e^{(b)} \rightarrow 0$  as  $n \rightarrow \infty$ .

In covert communication, one may additionally allow Alice and Bob to share a resource that is not accessible by the adversary. This can be a source of either classical randomness or quantum entanglement. Here, we focus on the former, that it, on covert communication that uses a pre-shared classical secret key  $k \in \mathcal{K}$  to randomize the encoder and, hence, the ensemble observed by the Willie [5], [7], [8]. Thus, in fact, Alice transmits  $\hat{\rho}_A^n(m, k)$  and Bob uses POVM  $\{\Lambda_{m,k}^n\}_{m \in \mathcal{M}}$ . However, we defer the analyses of the key size and the entanglement-assisted covert communication to future work.

2) *Sensing Model*: We study the covert version [9] of quantum-illumination-based binary target detection [19], depicted in Fig. 2b. Alice prepares an  $n$ -mode signal-reference state  $\hat{\rho}_{IS}^n$ . Alice retains reference ("idler") modes  $I$ . Signal modes  $S$  interrogate the target, modeled by a pure-loss bosonic channel  $\mathcal{E}_{S \rightarrow R'W'}^{\gamma^{(h)}, 0}$ , where transmittance to Willie  $\gamma^{(h)}$  depends on whether the target is absent ( $h = 0$ ,  $\gamma^{(0)} = 1$ ) or present ( $h = 1$ ,  $\gamma^{(1)} < 1$ ). Lossy thermal-noise bosonic channels  $\mathcal{E}_{R' \rightarrow R}^{\tau_A, \bar{n}_A}$  and  $\mathcal{E}_{W' \rightarrow W}^{\tau_W, \bar{n}_W}$  corrupt the light that the target reflects to Alice (modes  $R'$ ) and transmits to Willie (modes  $W'$ ), respectively. Note that one of the output modes in both channels is lost to the environment. Alice detects the presence of the target by performing a hypothesis test on the reference and returned modes  $I$  and  $R$  in the following quantum state:

$$\hat{\rho}_{IR}^n(h) = \left( \mathcal{I}_{I \rightarrow I} \otimes \mathcal{E}_{S \rightarrow R}^{(1-\gamma^{(h)})\tau_A, (1-\tau_A)\bar{n}_A} \right)^{\otimes n} (\hat{\rho}_{IS}^n), \quad (1)$$

where  $\mathcal{I}_{I \rightarrow I}$  is an identity channel and

$$\mathcal{E}_{S \rightarrow R}^{(1-\gamma^{(h)})\tau_A, (1-\tau_A)\bar{n}_A} = \mathcal{E}_{R' \rightarrow R}^{\tau_A, \bar{n}_A} \left( \text{tr}_{W'} \left[ \mathcal{E}_{S \rightarrow R'W'}^{\gamma^{(h)}, 0}(\hat{\rho}_S) \right] \right). \quad (2)$$

Note that, since probes are not returned when target is absent ( $h = 0$ ),  $\hat{\rho}_{IR}^n(h) = \text{tr}_S[\hat{\rho}_{IS}^n] \otimes \hat{\rho}_{th}^n((1-\tau_A)\bar{n}_A)^{\otimes n}$ , i.e., a product of reference and thermal states. Denote by  $H_0$  and  $H_1$  the respective hypotheses that the target is absent and present. For equal prior probabilities,

$\Pr(H_0 \text{ true}) = \Pr(H_1 \text{ true}) = 1/2$ , Alice's detection performance is quantified by the error probability  $P_e^{(s)} = \frac{P_{FA} + P_{MD}}{2}$ , where  $P_{FA} = \Pr(\text{choose } H_1 | H_0 \text{ true})$ , and  $P_{MD} = \Pr(\text{choose } H_0 | H_1 \text{ true})$ , and her task is to find a binary measurement and corresponding decision rule that minimizes  $P_e^{(s)}$ . The minimum achievable value is given by the Helstrom limit [20] [21, Sec. 9.1.4],

$$P_{e,\min}^{(s)} = \frac{1}{2} \left( 1 - \frac{1}{2} \|\hat{\rho}_{IR}^n(1) - \hat{\rho}_{IR}^n(0)\|_1 \right), \quad (3)$$

where  $\|\hat{A}\|_1 = \text{tr} \left[ \sqrt{\hat{A}^\dagger \hat{A}} \right]$  is the trace norm.

In both communication and active sensing, Alice's objective is to carry out her transmission while remaining undetected by the adversarial warden Willie. This requirement motivates the covertness criteria introduced next.

### B. Covertness criteria

Covertness is defined through Willie's ability to distinguish whether Alice is transmitting or not. When silent, she inputs innocent vacuum state  $\hat{\rho}_A^n = |0\rangle\langle 0|^{\otimes n}$ , which yields an  $n$ -mode thermal state at Willie,  $\hat{\rho}_{th}^{\otimes n}(\eta\bar{n}_B)$  for communication and  $\hat{\rho}_{th}^{\otimes n}((1-\tau_W)\bar{n}_W)$  for sensing.

Consider Alice transmitting in the communication setting. The  $n$ -mode state  $\hat{\rho}_W^n = \frac{1}{|\mathcal{M}|} \frac{1}{|\mathcal{K}|} \sum_{m,k} \text{tr}_W \left[ \left[ \mathcal{E}_{A \rightarrow BW}^{\eta, \bar{n}_B} \right]^{\otimes n} (\hat{\rho}_A^n(m, k)) \right]$  is Willie's output of channel  $\mathcal{E}_{A \rightarrow BW}^{\eta, \bar{n}_B}$  averaged over messages in  $\mathcal{M}$  and the secret from  $\mathcal{K}$  inaccessible by Willie. In the sensing setting, Willie's received state depends on the target:  $\hat{\rho}_{W,h}^n = \left( \mathcal{E}_{W' \rightarrow W}^{\tau_W, \bar{n}_W} \right)^{\otimes n} \left( \text{tr}_{IR'} \left[ \left( \mathcal{I}_{I \rightarrow I} \otimes \mathcal{E}_{S \rightarrow R'W'}^{\gamma^{(h)}, 0} \right)^{\otimes n} (\hat{\rho}_{IS}^n) \right] \right)$ , where  $h \in \{0, 1\}$  indicates target's presence.

As in [1], [2], we call a system covert if Willie's average detection error probability  $P_e^{(w)} \geq \frac{1}{2} - \delta$  for small  $\delta > 0$ . Like  $P_e^{(s)}$  in (3), it is bounded by expressions involving the trace distance. For communication it is:

$$P_e^{(w)} \geq \frac{1}{2} \left( 1 - \frac{1}{2} \|\hat{\rho}_W^n - \hat{\rho}_{th}^{\otimes n}(\eta\bar{n}_B)\|_1 \right), \quad (4)$$

whereas for sensing it is:

$$P_e^{(w)} \geq \frac{1}{2} \left( 1 - \max_{h \in \{0, 1\}} \frac{1}{2} \|\hat{\rho}_{W,h}^n - \hat{\rho}_{th}^{\otimes n}((1-\tau_W)\bar{n}_W)\|_1 \right). \quad (5)$$

Numerical evaluation suggests that the target-absent case ( $h = 0$ ) minimizes the lower bound in (5); we defer confirming this analytically to future work. The trace distance is often mathematically inconvenient, however the quantum relative entropy (QRE) upper bounds it via the quantum Pinsker's inequality [21, Th. 11.9.1]:  $\frac{1}{2} \|\hat{\rho} - \hat{\sigma}\|_1 \leq \sqrt{\frac{1}{2} D(\hat{\rho} \|\hat{\sigma})}$ . QRE is also additive over the product states. Therefore, as is common practice in the covertness literature [5], [7], [9], [22], [23], we use it to define our covertness constraint directly: the communication and sensing systems are covert if:

$$\max_{h \in \{0,1\}} D(\hat{\rho}_{W,h}^n \|\hat{\rho}_{\text{th}}^{\otimes n}((1-\tau_W)\bar{n}_W)) \leq \delta_{\text{QRE}}. \quad (6)$$

Setting  $\delta_{\text{QRE}} = 8\delta^2$  meets the constraints in (4) and (5).

### C. Signaling Scheme

This covertness criterion requires the average transmitted energy per mode to scale as  $\frac{1}{\sqrt{n}}$  [1], [2]. In the sparse signaling scheme considered next, this scaling is achieved by letting the fraction of active modes  $\alpha$  to vanish as  $n \rightarrow \infty$ .

As previous research studied, in covert communication and sensing, signaling schemes are classified according to how transmission activity is distributed across channel uses. Under a covertness constraint, Alice must ensure that the induced change at Willie is sufficiently small. Broadly speaking, Alice may either distribute a weak signal over essentially all channel uses, or instead transmit only rarely while keeping most uses identical to vacuum. These two schemes are called diffuse signaling and sparse signaling, respectively.

In diffuse signaling, the Alice employs nearly every channel use, but with very low per-use energy. Covertness is then maintained by ensuring that each individual use produces only a slight difference relative to the innocent background. This signaling regime was studied heavily in [9]. However, in radio frequency covert communication, finite data converter resolution and synchronization constraints make sparse signaling experimentally important and practical [10].

Therefore, our focus is on sparse signaling. In this scheme, the transmitter remains silent for most channel uses and only occasionally sends a nontrivial signal state. We can describe the ensemble-averaged single-mode input state by assigning a vanishing probability  $\alpha$  to the active input signal state  $\hat{\rho}_A$  and probability  $1 - \alpha$  to the innocent input vacuum state  $|0\rangle\langle 0|$ , with  $0 < \alpha < 1$ .

$$\hat{\rho}_{\text{sp}} = (1 - \alpha)\hat{\rho}_{\text{th}}(0) + \alpha\hat{\rho}_A, \quad (7)$$

After  $\hat{\rho}_{\text{sp}}$  goes through the lossy thermal-noise channel  $\mathcal{E}_{A \rightarrow BC}^{\eta, \bar{n}_B}$  described earlier, the ensemble-averaged single-mode output state Willie observed is a sparse state of the form

$$\hat{\rho}_\alpha = (1 - \alpha)\hat{\rho}_{\text{th}}(\eta\bar{n}_B) + \alpha\hat{\rho}_W, \quad (8)$$

where

$$\hat{\rho}_\alpha(\eta\bar{n}_B) = \sum_{\ell=0}^{\infty} \lambda_\ell |\ell\rangle\langle \ell|, \quad \lambda_\ell = \frac{(\eta\bar{n}_B)^\ell}{(1 + \eta\bar{n}_B)^{\ell+1}}, \quad (9)$$

is the attenuated thermal output state and  $\hat{\rho}_W$  is the output state induced by the active input, and over  $n$  i.i.d modes his average state is  $\hat{\rho}_{W,\alpha}^n = \hat{\rho}_\alpha^{\otimes n}$ . Over  $n$  modes, the sparse signaling model describes transmission on a vanishing fraction of modes  $\alpha$  with fixed input mean photon number  $\bar{n}_S$ , while the remaining modes are kept in the vacuum state. This sparse-mixture is the structure is the foundation for our optimization of covert signaling states.

## III. CHARACTERIZATION OF SPARSE SIGNALING

In sparse signaling the input state mean photon number  $\bar{n}_S$  is fixed and covertness is achieved through the vanishing transmission probability  $\alpha$ . Now, because the state seen by Willie is a convex mixture of the innocent and active states, so the QRE-covert criteria is governed by its behavior in  $\alpha$  rather than by the signal energy or a physical channel parameter. Inspired by the QRE perturbation framework of [24], we proceed through a data-processing argument that is well suited to the infinite-dimensional bosonic setting. We apply the data-processing inequality for QRE to the sparse output state  $\hat{\rho}_\alpha$  in (8) to show that the covertness minimizer may be chosen to be diagonal in the Fock basis under mean photon number constraint  $\text{tr}(\hat{\rho}_A \hat{N}) = \bar{n}_S$ . The main result shows that the minimizer is supported on at most two consecutive Fock states.

### A. Optimal Input State under Sparse Signaling

**Definition III.1.** (Phase rotation unitary). With number operator  $\hat{N} = a^\dagger a$ , where  $a$  is the complex amplitude of input mode function. The phase-rotation unitary

$$U_\phi = e^{-i\phi\hat{N}}, \quad \phi \in [0, 2\pi). \quad (10)$$

**Definition III.2** (Dephasing channel).

$$\Delta(\hat{\rho}) = \sum_{\ell=0}^{\infty} |\ell\rangle\langle \ell| \hat{\rho} |\ell\rangle\langle \ell|. \quad (11)$$

Equivalently,

$$\Delta(\hat{\rho}) = \int_0^{2\pi} e^{i\phi\hat{N}} \hat{\rho} e^{-i\phi\hat{N}} \frac{d\phi}{2\pi}. \quad (12)$$

Thus the dephasing channel removes the off-diagonal entries of  $\hat{\rho}$  in the Fock basis and resulting an Fock-diagonal state. Since  $\hat{\rho}_{\text{th}}(\eta\bar{n}_B)$  is diagonal in the Fock basis,  $\Delta(\hat{\rho}_{\text{th}}(\eta\bar{n}_B)) = \hat{\rho}_{\text{th}}(\eta\bar{n}_B)$ . Also, dephasing preserves the mean photon number:  $\text{tr}[\Delta(\hat{\rho}_A)\hat{N}] = \text{tr}[\hat{\rho}_A\hat{N}]$ .

**Definition III.3.** (Phase covariant channel) A channel  $\mathcal{N}_{A \rightarrow B}$  is phase-covariant if,

$$\mathcal{N}_{A \rightarrow B}(U_\phi \hat{\rho} U_\phi^\dagger) = U_\phi \mathcal{N}_{A \rightarrow B}(\hat{\rho}) U_\phi^\dagger \quad \forall \phi. \quad (13)$$

where  $\mathcal{N}_{A \rightarrow B}$  is a linear, completely positive, and trace-preserving (CPTP) map.

The thermal-lossy channel are the dephasing channel are phase covariant [25], [26]. The arguments are that lossy thermal-noise channel commutes with phase rotations and because the channel loss interaction and the thermal noise are phase-insensitive, Similarly, the Fock-basis dephasing channel

is phase covariant because it is defined by photon-number basis  $|\ell\rangle\langle\ell|$ , which are invariant under phase rotations.

We now state the primary result of this section.

**Theorem 1** (Optimal sparse input state structure). For any single-mode quantum input state with mean photon number  $\bar{n}_S$ , the sparse QRE second-order coefficient is minimized by an Fock-diagonal state supported on at most two consecutive Fock states. Specifically, let  $\kappa = \lfloor \bar{n}_S \rfloor$ , then there exists an optimizer of the form  $\hat{\rho}_{A,\text{opt}} = \sum_{i \geq 0} \rho_i |i\rangle\langle i|$ , with  $\rho_\kappa = \kappa + 1 - \bar{n}_S$ ,  $\rho_{\kappa+1} = \bar{n}_S - \kappa$ , and  $\rho_i = 0$  for all  $i \notin \{\kappa, \kappa + 1\}$ . More explicitly,

$$\hat{\rho}_{A,\text{opt}} = (\kappa + 1 - \bar{n}_S) |\kappa\rangle\langle\kappa| + (\bar{n}_S - \kappa) |\kappa + 1\rangle\langle\kappa + 1|. \quad (14)$$

*Proof: Construction:*

The proof is developed through the sequence of results below. We first show that, after data processing under dephasing, the optimization may be restricted to Fock-diagonal input states. Then, we derive the corresponding Willie-side perturbation coefficient  $C_P$  explicitly. Hence, the sparse-covertness problem reduces to minimizing  $C_P$  over the input distribution  $\rho_i$ . Next, We exploit orthogonal structure of  $C_P$  which exposes its dependence on the input factorial moments. Finally, combining this representation with a discrete-convexity argument yields an optimizer supported on at most two consecutive Fock states. The detailed steps are given in sec III-B, lemmas 1–4 and the resulting corollary 1.

*B. Dephasing reduction*

For sparse signaling, the QRE-covert criteria is

$$D(\hat{\rho}_\alpha \| \hat{\rho}_{\text{th}}(\eta \bar{n}_B)) \quad (15)$$

The goal is to minimize this quantity and find a potential minimizer input state under the mean photon constraint. Note that, since lossy thermal-noise channel and dephasing channel are both phase covariant, dephasing before thermal loss at Alice's sparse input state  $\hat{\rho}_{\text{sp}}$  is equivalent to dephasing after the channel at Willie's sparse output state  $\hat{\rho}_\alpha$ ,

$$\begin{aligned} \Delta(\hat{\rho}_\alpha) &= (1 - \alpha)\Delta(\hat{\rho}_{\text{th}}(\eta \bar{n}_B)) + \alpha\Delta(\hat{\rho}_W) \\ &= \Delta(\mathcal{E}_{A \rightarrow BC}^{\eta, \bar{n}_B}(\hat{\rho}_{\text{sp}})) \\ &= (1 - \alpha)\mathcal{E}_{A \rightarrow BC}^{\eta, \bar{n}_B}(\Delta(|0\rangle\langle 0|)) + \alpha\mathcal{E}_{A \rightarrow BC}^{\eta, \bar{n}_B}(\Delta(\hat{\rho}_A)). \end{aligned} \quad (16)$$

and using the fact that  $\hat{\rho}_{\text{th}}$  is diagonal in the Fock basis, so it is dephasing invariant,  $\Delta(\hat{\rho}_{\text{th}}) = \hat{\rho}_{\text{th}}$ . Now, by the data-processing inequality for QRE,

$$D(\hat{\rho}_\alpha \| \hat{\rho}_{\text{th}}(\eta \bar{n}_B)) \geq D(\Delta(\hat{\rho}_\alpha) \| \Delta(\hat{\rho}_{\text{th}}(\eta \bar{n}_B))). \quad (17)$$

Substitute (16) into (17) Concluding,

$$D(\hat{\rho}_\alpha \| \hat{\rho}_{\text{th}}(\eta \bar{n}_B)) \geq D(\mathcal{E}_{A \rightarrow BC}^{\eta, \bar{n}_B}(\Delta(\hat{\rho}_{\text{sp}})) \| \hat{\rho}_{\text{th}}(\eta \bar{n}_B)), \quad (18)$$

Thus, for every feasible input state  $\hat{\rho}_A$ , the Fock-diagonal input  $\Delta(\hat{\rho}_A)$  is also feasible and gives Willie a QRE no larger than the original one. Therefore, there is no loss of optimality in restricting the covertness minimization under mean photon constraint  $\text{tr}[\hat{\rho}_A \hat{N}]$  to Fock-diagonal inputs.

*C. QRE diagonal perturbation expansion*

We now consider a single bosonic mode  $A$  at the channel input, prepared in a diagonal state supported on the truncated Fock subspace  $\mathcal{H}_j = \text{span}\{|0\rangle, |1\rangle, \dots, |j\rangle\}$ . The mode  $A$  propagates through a thermal lossy bosonic channel that mix the input with an environment mode  $E$  in a thermal state. We derive the output state seen by Willie in the Fock diagonal basis by producing the characteristic function inversion.

**Lemma 1** (Willie's active output photon-number distribution). Let  $\hat{\rho}_A = \sum_{i=0}^j \rho_i |i\rangle\langle i|$ , with  $\rho_i \geq 0$  and  $\sum_{i=0}^j \rho_i = 1$ . Suppose that the input state passes through a thermal lossy bosonic channel,  $\mathcal{E}_{A \rightarrow BC}^{\eta, \bar{n}_B}$ . Then Willie's output state is diagonal in the Fock basis and can be written as

$$\hat{\rho}_W = \sum_{\ell=0}^{\infty} p_\ell |\ell\rangle\langle\ell|. \quad (19)$$

Moreover, for every  $\ell \geq 0$ , the output photon-number probability  $p_\ell$  admits the integral representation

$$p_\ell = \sum_{i=0}^j \rho_i \int_0^\infty e^{-(1+\eta\bar{n}_B)x} L_\ell(x) L_i((1-\eta)x) dx, \quad (20)$$

where  $L_n(\cdot)$  denotes the Laguerre polynomial of degree  $n$ . Equivalently,  $p_\ell$  admit the explicit finite-sum representation

$$p_\ell = \sum_{i=0}^j \rho_i \sum_{t=0}^i \sum_{u=0}^{\ell} (-1)^{t+u} \binom{i}{t} \binom{\ell}{u} (1-\eta)^t \frac{(t+u)!}{t! u!} \frac{1}{(1+\eta\bar{n}_b)^{t+u+1}}. \quad (21)$$

The proof relies on the characteristic-function description of the lossy thermal-noise channel. Specifically, we first express Willie's output characteristic function through the beam-splitter input–environment decomposition and show that, for a Fock-diagonal truncated input, the input dependence is captured by Laguerre polynomials. We then invert the characteristic function in the Fock basis; after converting to polar coordinates, the angular integration forces the off-diagonal matrix elements to vanish, which establishes the diagonal form of Willie's output and yields the integral formula for its photon-number distribution. Finally, a term-by-term expansion of the Laguerre polynomials leads directly to the closed-form finite-sum representation. The full proof is given in Appendix I.

As a consequence of the diagonal form of Willie's active output, the Willie-side sparse QRE admits the following explicit second-order expression.

**Lemma 2** (Second-order expansion of sparse QRE). Let the sparse state (8) be  $\hat{\rho}_\alpha = (1 - \alpha)\hat{\rho}_{\text{th}}(\eta \bar{n}_B) + \alpha\hat{\rho}_W$ , where  $\hat{\rho}_W$  the active Willie's output state is diagonal in the Fock basis (Lemma 1),  $\hat{\rho}_W = \sum_{\ell=0}^{\infty} p_\ell |\ell\rangle\langle\ell|$ . Then, the Willie-side QRE admits the expansion

$$D(\hat{\rho}_\alpha \| \hat{\rho}_{\text{th}}(\eta \bar{n}_B)) = \frac{\alpha^2}{2} C_W + o(\alpha^2), \quad (22)$$

Where  $C_W$  is the QRE coefficient for corresponding general input states. For the state in (19)  $C_W$  is the perturbation coefficient  $C_P$

$$C_P = \sum_{\ell=0}^{\infty} \frac{(p_\ell - \lambda_\ell)^2}{\lambda_\ell}, \quad (23)$$

and  $p_\ell$  is expressed in (20) and (21).

The proof of lemma 2 is straightforward. Since  $\hat{\rho}_\alpha$  and  $\hat{\rho}_{\text{th}}(\eta\bar{n}_B)$  commutes, the QRE reduces to a classical Kullback-Leibler (KL) divergence. Hence, the problem becomes a scalar second order Taylor expansion. The detailed derivation is in Appendix II

#### D. Orthogonal Structural Optimization

The representation of the perturbation coefficient  $C_P$  in lemma 2 is explicit, but it is not yet for clear structural analysis or optimization. Indeed, in (23),  $C_P$  is expressed through the output photon number probabilities  $p_\ell$ , and each  $p_\ell$  depends on the entire input distribution through the lossy thermal channel. As a result, the contribution of a given input Fock component is spread across all output photon numbers, and the dependence of  $C_P$  on  $\rho_i$  is hidden inside a complicated expression, which makes it difficult to identify which features of the input state increase detectability at Willie. To obtain a more informative characterization, we next derive an orthogonal representation of  $C_P$ . This representation rewrites the same perturbation coefficient as a weighted sum of squares of input-dependent moment quantities. In particular, it exposes how the photon number structure is penalized, and provides the key tool for proving the sparse optimal-input structure established in Theorem 1.

**Definition III.4** (Meixner polynomials). (See [27, Section 1.1.9]) For  $0 < q < 1$ , the Meixner polynomials  $\{M_y(\ell; q)\}_{y \geq 0}$  are defined for  $\ell, y \in \{0, 1, 2, \dots\}$  by the hypergeometric function

$$M_y(\ell; q) = {}_2F_1\left(\begin{matrix} -y, -\ell \\ 1 \end{matrix}; 1 - \frac{1}{q}\right). \quad (24)$$

Equivalently, they are characterized by the generating function

$$\sum_{y=0}^{\infty} M_y(\ell; q) \nu^y = \left(1 - \frac{\nu}{q}\right)^\ell (1 - \nu)^{-\ell-1}, \quad |\nu| < 1. \quad (25)$$

Moreover, they are orthogonal with respect to the geometric distribution  $\lambda_\ell = (1 - q)q^\ell$ , namely

$$\sum_{\ell=0}^{\infty} \lambda_\ell M_y(\ell; q) M_{y'}(\ell; q) = q^{-y} \delta_{y, y'}. \quad (26)$$

**Lemma 3.** (Orthogonal form of  $C_P$ ) For Fock-diagonal input states, Willie's one-mode output is also diagonal in the Fock-basis, and the sparse-QRE perturbation coefficient admits an orthogonal representation:

$$C_P = \sum_{y=1}^j q^{-y} \theta^{2y} \mu_y^2, \quad (27)$$

where

$$\mu_y = \sum_{i=y}^j \rho_i \binom{i}{y}, \quad (28)$$

and

$$q = \frac{\eta\bar{n}_B}{1 + \eta\bar{n}_B}, \quad \theta = \frac{1 - \eta}{1 + \eta\bar{n}_B}. \quad (29)$$

The proof proceeds by rewriting the coefficient  $C_P$  from lemma 2 in a form that makes its dependence on the input distribution explicit. Starting from the expression for Willie's output photon-number probabilities (20), we first write  $C_P$  as a quadratic form with respect to the thermal photon-number distribution. Since  $\lambda_\ell$  is geometric, the Meixner polynomials provide the natural orthogonal basis for the analysis. We then derive an expansion of the normalized coefficients in this basis by comparing generating functions, which expresses the deviation  $\frac{p_\ell}{\lambda_\ell} - 1$  in terms of input-dependent factorial moments. Finally, substituting this expansion into  $C_P$  and invoking Meixner orthogonality removes all cross terms, thereby yielding the orthogonal representation in (27). The complete proof is given in Appendix III.

Lemma 3 shows that the perturbation coefficient  $C_P$  can be decomposed into an explicit function of the input photon-number distribution  $\{\rho_i\}$ . This representation makes the optimization problem transparent: under the normalization and mean-photon-number constraint  $\sum_{i=1}^j i\rho_i = \bar{n}_S$ , the first factorial moment  $\mu_1$  is fixed by  $\bar{n}_S$ , so minimizing  $C_P$  reduces to suppressing the higher-order factorial moment  $y \geq 2$ . The problem is therefore reduced to a discrete moment allocation over  $\{\rho_i\}$ , and this structure allows an optimization based on the convexity of the binomial moments. As we show next, this yields an optimizer supported on at most two consecutive Fock states.

**Definition III.5** (Discrete convexity). (See [28, page 42, Ex.1]) A function  $\varphi : \mathbb{Z}_{\geq 0} \rightarrow \mathbb{R}$  is discrete convex if for every  $i \geq 0$

$$\varphi(i+2) - 2\varphi(i+1) + \varphi(i) \geq 0. \quad (30)$$

Equivalently, the increments  $\varphi(i+1) - \varphi(i)$  are nondecreasing in  $i$ .

**Lemma 4.** (Two-point lower bound) Let  $\varphi$  be discrete convex and let  $I$  be any integer-valued random variable with mean  $\mathbb{E}[I] = \kappa + \beta$ ,  $\kappa = \lfloor \mathbb{E}[I] \rfloor$ ,  $\beta \in [0, 1)$ . Then

$$\mathbb{E}[\varphi(I)] \geq (1 - \beta) \varphi(\kappa) + \beta \varphi(\kappa + 1), \quad (31)$$

and equality holds when  $\Pr[I = \kappa] = 1 - \beta$  and  $\Pr[I = \kappa + 1] = \beta$ .

We refer the detailed proof of Lemma 4 in Appendix IV. To apply Lemma 4 in our setting, fix  $y \geq 2$  and define  $\varphi_y(i) = \binom{i}{y}$  for  $i \in \mathbb{Z}_{\geq 0}$ . Then  $\varphi_y$  is discrete convex, since two successive applications of Pascal's identity  $\binom{i+1}{y} = \binom{i}{y} + \binom{i}{y-1}$  give

$$\binom{i+2}{y} - 2\binom{i+1}{y} + \binom{i}{y} = \binom{i}{y-2} \geq 0. \quad (32)$$

Hence each factorial moment  $\mu_y = \sum_{i \geq y} \rho_i \binom{i}{y}$  falls within Lemma 4.

**Corollary 1** (Consecutive-support optimizer). Let  $\bar{n}_S = \kappa + \beta$ , where  $\kappa = \lfloor \bar{n}_S \rfloor$  and  $\beta \in [0, 1)$ . Under the normalization and mean-photon-number constraints  $\sum_{i \geq 0} \rho_i = 1$ ,  $\sum_{i \geq 0} i \rho_i = \bar{n}_S$ , an optimizer of the Willie-side perturbation coefficient  $C_P$  in Lemma 3 can be taken to be supported on the two consecutive Fock numbers  $\kappa$  and  $\kappa + 1$ . More precisely, there exists an optimizer of the form

$$\rho_\kappa = 1 - \beta, \quad \rho_{\kappa+1} = \beta, \quad \rho_i = 0 \quad \text{for } i \notin \{\kappa, \kappa + 1\}. \quad (33)$$

By Lemma 3,  $C_P = \sum_{y=1}^j q^{-y} \theta^{2y} \mu_y^2$ , with strictly positive coefficients  $q^{-y} \theta^{2y}$ . The first factorial moment is fixed by the mean-photon-number constraint, since  $\mu_1 = \sum_{i \geq 1} i \rho_i = \bar{n}_S$ . Thus minimizing  $C_P$  over the distribution  $\rho_i$  reduces to minimizing  $\mu_y$  for all  $y \geq 2$ . For each such  $y$ , the function  $\binom{i}{y}$  is discrete convex by (32). Lemma 4 therefore implies

$$\mu_y \geq (1 - \beta) \binom{\kappa}{y} + \beta \binom{\kappa + 1}{y}, \quad y \geq 2,$$

with equality for the two-point distribution in (33). Hence this distribution minimizes every higher-order factorial moment simultaneously, and therefore minimizes  $C_P$ .

Theorem 1 now follows by combining the preceding steps. Section III-B show that an optimizer can be taken to be Fock-diagonal. Lemma 1 and Lemma 2 identify the corresponding sparse-QRE perturbation coefficient, while Lemma 3 rewrites it as a positive sum of squared factorial moments of the input photon-number distribution. Applying Lemma 4 to the discrete-convex sequence  $\binom{i}{y}$ ,  $y \geq 2$ , shows that these higher-order moments are minimized by a distribution supported on two consecutive Fock states; Corollary 1 gives this optimizer explicitly as the allocation on  $\{\kappa, \kappa + 1\}$ , where  $\kappa = \lfloor \bar{n}_S \rfloor$ . This is exactly the structure claimed in Theorem 1. ■

We now turn to the low-brightness covert setting. In this case, the optimal sparse input reduces to a mixture of only the vacuum and single-photon states, which makes the structure especially transparent.

#### IV. IMPLICATIONS IN THE COVERT REGIME

In this section we analyze the impact of the optimal sparse input state on the low-photon-number regime  $0 \leq \bar{n}_S \leq 1$ . Although covertness is imposed throughout via the Willie-side QRE constraint, in covert communication and sensing, the mean transmitted photon number per mode scales as  $O(\sqrt{\delta/\bar{n}})$  [7], [9]. Thus, under sparse signaling asymptotically, the covert constraint forces  $\alpha$  to vanish with  $n$ , and therefore making  $\alpha \bar{n}_S$  vanishing asymptotically as  $n$  grows. We therefore focus here on the low-brightness regime, which can be interpreted within the same small fixed  $\delta$  constrained covert signaling problem. We show that the low-brightness optimal sparse input  $\hat{\rho}_{A,\text{opt}}$  is the optimizer of the sparse perturbation coefficient  $C_P$ , it saturates the converse minimal for covert communication [7, Thm.1], and it matches the optimal sensing diffuse TMSV covertness criteria [9] in the following corollaries.

##### A. Low-Brightness Sparse Optimum

We begin by apply the main theorem of Section III to the low-brightness regime.

**Corollary 2** (Optimal sparse input for low-brightness regime). For  $0 \leq \bar{n}_S \leq 1$ , the optimal sparse input state is

$$\hat{\rho}_{A,\text{cov}} = (1 - \bar{n}_S) |0\rangle\langle 0| + \bar{n}_S |1\rangle\langle 1|. \quad (34)$$

*Proof:* This follows immediately from Theorem 1. Indeed, for  $0 \leq \bar{n}_S \leq 1$ , we have  $\kappa = \lfloor \bar{n}_S \rfloor = 0$ , so the optimal input state in (14) reduces to (34). At the endpoint  $\bar{n}_S = 1$ , the same expression yields the pure one-photon state  $|1\rangle\langle 1|$ . ■

Corollary 2 shows that the sparse covert optimizer in the low-brightness regime is a very simple non-Gaussian state. Thus, in the regime most relevant to covert operation, the active input that minimizes Willie's detectability is a sharply concentrated photon-number allocation on vacuum and one photon state. This observation will underlie all of the comparisons that follow.

##### B. Covert Communication Converse Saturation

Since the QRE is additive over product state, from (22) and (23), this yield

$$D\left(\hat{\rho}_{W_\alpha}^n \left\| \hat{\rho}_{\text{th}}(\eta \bar{n}_B)^{\otimes n}\right.\right) = \frac{n\alpha^2}{2} C_P + o(\alpha^2) \quad (35)$$

The following lemma 5 and corollary 3 show that optimal input state  $\hat{\rho}_{\alpha,\text{cov}}$  matches the converse minimal for covert communication at quadratic order.

**Lemma 5** (Bosonic covert converse). [7, Thm. 1] Any scheme whose Willie-side QRE must satisfy

$$D\left(\hat{\rho}_W^n \left\| \hat{\rho}_{\text{th}}(\eta \bar{n}_B)^{\otimes n}\right.\right) \geq \frac{n}{2} \frac{(1 - \eta)^2}{\eta \bar{n}_B (1 + \eta \bar{n}_B)} \bar{n}_{\text{msg}}^2 + o(\bar{n}_{\text{msg}}^2) \quad (36)$$

where  $\bar{n}_{\text{msg}}$  is the mean transmitted photon number per mode, averaged over the size of message set  $|\mathcal{M}|$ . This is a well-known result from [7]. We refer the detailed derivation to [7, Thm. 1].

**Corollary 3** (Converse saturation in the low-brightness regime). For  $0 \leq \bar{n}_S \leq 1$ , the optimal sparse input in Corollary 2 yields

$$\begin{aligned} D\left(\left(\hat{\rho}_{\alpha,\text{cov}}\right)^{\otimes n} \left\| \hat{\rho}_{\text{th}}(\eta \bar{n}_B)^{\otimes n}\right.\right) \\ = \frac{\alpha^2 n}{2} \frac{(1 - \eta)^2}{\eta \bar{n}_B (1 + \eta \bar{n}_B)} \bar{n}_S^2 + o(\alpha^2), \end{aligned} \quad (37)$$

and therefore attains the converse-minimal Willie-side perturbation coefficient in Lemma 5.

*Proof:* From Corollary 2, the photon distribution allocations are  $\rho_0 = 1 - \bar{n}_S$ ,  $\rho_1 = \bar{n}_S$ , and  $\rho_i = 0$  for  $i \geq 2$ , substitute into the perturbation coefficient formula (27) in Lemma 3. This gives  $\mu_1 = \sum_{i \geq 1} i \rho_i = \bar{n}_S$ , while for every  $y \geq 2$ ,  $\mu_y = 0$ . Therefore only the  $y = 1$  term survives in (27), and hence  $C_P = q^{-1} \theta^2 \bar{n}_S^2$ . Now, using the definitions (29) of  $q, \theta$ , plug into the expansion of QRE

(22)  $D(\hat{\rho}_\alpha \| \hat{\rho}_{\text{th}}(\eta \bar{n}_B)) = \frac{\alpha^2}{2} C_P + o(\alpha^2)$ , and identifying for sparse signaling,  $\bar{n}_{\text{msg}} = \alpha \bar{n}_S$  asymptotically. The saturation of Lemma 5 follows intermediately. ■

### C. Optimality for Covert Sensing

We compare the diffuse signaling scheme from [9]. In this case, Alice prepares  $n$  independent two-mode squeezed vacuum (TMSV) pairs. She then sends a weak signal in every mode, rather than sending a stronger signal in only a small fraction of modes. For a single-mode,

$$|\text{TMSV}\rangle = \sum_{i=0}^{\infty} \sqrt{\frac{\bar{n}_S^i}{(1 + \bar{n}_S)^{i+1}}} |i\rangle_S |i\rangle_I. \quad (38)$$

Then Alice transmit the thermal signal marginal, by taking the partial trace over the reference mode,

$$\hat{\rho}_{S, \text{TMSV}} = \text{tr}_I |\text{TMSV}\rangle \langle \text{TMSV}| = \sum_{i=0}^{\infty} \frac{\bar{n}_S^i}{(1 + \bar{n}_S)^{i+1}} |i\rangle \langle i|. \quad (39)$$

After it passes through Willie's effective lossy thermal-noise channel, he receives,

$$\begin{aligned} \hat{\rho}_{W, \text{diff}} &= \mathcal{E}^{(\gamma^{(h)})\tau_W, (1-\tau_W)\bar{n}_W}(\hat{\rho}_A) \\ &= \sum_{\ell=0}^{\infty} \frac{(\gamma^{(h)}\tau_W\bar{n}_S + (1-\tau_W)\bar{n}_W)^\ell}{(1 + \gamma^{(h)}\tau_W\bar{n}_S + (1-\tau_W)\bar{n}_W)^{\ell+1}} |\ell\rangle \langle \ell|, \end{aligned} \quad (40)$$

with mean photon number,  $\gamma^{(h)}\tau_W\bar{n}_S + (1-\tau_W)\bar{n}_W$ .

Now we adopt the diffuse covertness result [9] as a lemma:

**Lemma 6** (Diffuse TMSV QRE). In the diffuse scheme, Alice sends one TMSV probe in every mode, with per-mode signal mean photon number  $\bar{n}_S$ . Then Willie's single-mode quantum relative entropy satisfies

$$D(\hat{\rho}_{W, \text{diff}}^{\otimes n} \| \hat{\rho}_{\text{th}}^{\otimes n}) = \frac{(\tau_W\bar{n}_S)^2}{2(1-\tau_W)\bar{n}_W(1+(1-\tau_W)\bar{n}_W)} + o(n_S^2). \quad (41)$$

We refer the detailed derivation of Lemma 6 to [9, Sec 3.1].

**Corollary 4** (Diffuse TMSV Matches Sparse  $\hat{\rho}_{A, \text{cov}}$ ). Under matched transmitted mean photon number, for  $0 \leq \bar{n}_S \leq 1$ , the sensing diffuse TMSV scheme and the optimal sparse input  $\hat{\rho}_{A, \text{cov}}$  in corollary 2 have the same Willie-side quadratic QRE coefficient,

$$C_{\text{diff}} = \frac{\tau_W^2}{(1-\tau_W)\bar{n}_W(1+(1-\tau_W)\bar{n}_W)}. \quad (42)$$

where  $C_{\text{diff}}$  is the diffuse TMSV Willie-side QRE coefficient.

*Proof:* First, in sparse signaling, the expansion is taken with respect to  $\alpha$ , with the input mean photon number  $\bar{n}_S$  fixed. Hence the Willie-side QRE coefficient is proportional to  $\alpha^2 \bar{n}_S^2$ , instead of just  $\bar{n}_S$  for diffuse signaling shown in lemma 6. Next, from the proof of corollary 3 after plug in the optimal photon distribution allocation in corollary 2 the perturbation coefficient reduced to  $C_P = q^{-1} \theta^2 \bar{n}_S^2$ . Note

that, in the sensing model, the transitivity is  $\tau_W$  and the attenuated thermal mean photon number at Willie's receiver under target absence is  $(1-\tau_W)\bar{n}_W$ . Hence, in the sensing model,  $q = \frac{(1-\tau_W)\bar{n}_W}{1+(1-\tau_W)\bar{n}_W}$  and  $\theta = \frac{\tau_W}{1+(1-\tau_W)\bar{n}_W}$ . Corollary 4 follows immediately, after the substitution of  $q$  and  $\theta$ . ■

These equivalences show that, in the low-brightness regime, the covert penalty has been minimized, the comparison between communication-oriented and sensing-oriented signaling strategies is therefore driven primarily by the corresponding functionality terms. In the next section, this perspective is discussed.

## V. SPARSE SIGNALING PERFORMANCE ANALYSIS OF COVERT COMMUNICATION AND SENSING

The results of Sections III and IV characterize the sparse input state that minimizes the covert criteria. For general input states, we denote the corresponding QRE coefficient by  $C_W$ . We now quantify the operational implications of this covertness optimization for communication and sensing. By the additive property of QRE and impose the covertness constraint,  $D(\hat{\rho}_\alpha^{\otimes n} \| \hat{\rho}_{\text{th}}^{\otimes n}) = n D(\hat{\rho}_\alpha \| \hat{\rho}_{\text{th}}) = \frac{n\alpha^2}{2} C_W + n o(\alpha^2) \leq \delta$ . Hence,  $\alpha$  scale as  $\sqrt{\frac{2\delta}{nC_W}}$  under the covertness budget  $\delta$ , so the covert performance takes the form  $(\alpha\sqrt{n})$  multiplied by the relevant functionality term. We now relate these functionality metrics to the probability of error introduced in Section II-A. For communication, the relevant performance quantity is the number of messages that can be transmitted while ensuring that Bob's average decoding error probability  $P_e^{(b)}$  vanishes as  $n \rightarrow \infty$ . Thus, the mutual information or Holevo information determines the largest reliable message size under the covertness constraint. For sensing, the Chernoff exponent directly controls the decay rate of Alice's minimum target-detection error probability  $P_e^{(s)}$ . Therefore, the performance metrics should be interpreted as square-root-law coefficients: in communication, they determine the number of reliably transmissible bits per  $\sqrt{n}$ ; in sensing, they determine the exponent governing the decay of  $P_e^{(s)}$  on the  $\sqrt{n}$  scale. Hence, for sparse signaling, the covert system capabilities are governed by a tradeoff between the QRE coefficient  $C_W$ , which fixes  $\alpha$  under the covertness constraint  $\delta$ , and the corresponding functionality metric: the information-transmission capacities for communication or the Chernoff exponents for sensing.

For the covertness-optimized signaling strategy, both communication and sensing use the optimal sparse Fock-diagonal input from Corollary 2. The resulting intended output states are therefore Fock-diagonal: in sensing, the states for target absence and presence are diagonal in the Fock basis, while in communication the OFF and ON output states at Bob are diagonal in the same basis. Since these states commute, photon-number-resolving (PNR) detection is optimal for the corresponding reduced decision problem [20], and the resulting performance metrics can be written directly in terms of classical photon-count distributions.

The numerical results in Figs. 3 and 4 compare the covert communication and sensing capabilities as functions of  $\bar{n}_S$ . Motivated by [29], [30], the parameter values of transmissivity and background thermal photon numbers are relevant

to photon-starved free-space optical (FSO) communication with noisy receiver and low-background with moderate-return optical active sensing. The resulting crossovers illustrate the central tradeoff in sparse covert signaling: at small  $\bar{n}_S$ , schemes optimized for communication or sensing performance may be superior, whereas at larger  $\bar{n}_S$ , the QRE perturbation coefficient achieved by the covertness-optimal input can become dominant.

### A. Covert Communication Performance

It is convenient to introduce  $X \in \{0, 1\}$ ,  $\Pr(X = 1) = \alpha$ ,  $\Pr(X = 0) = 1 - \alpha$ , where  $X = 0$  corresponds to the OFF symbol and  $X = 1$  corresponds to the ON symbol. Alice then uses the covertness-optimal Fock-diagonal state from Corollary 2. Since Alice transmits the ON symbol with probability  $\alpha$  and remains silent with probability  $1 - \alpha$ , Bob observes an induced classical binary asymmetric channel. Its output is the photon number detected by Bob, so the output alphabet is  $\mathcal{Y} = \{0, 1, 2, \dots\}$ , with  $Y = \ell$  corresponding to the detection of  $\ell$  photons. We denote the two transition probabilities of the asymmetric channel by  $p_{Y|X}(\ell|0)$  and  $p_{Y|X}(\ell|1)$ , corresponding respectively to  $|0\rangle\langle 0|$  and  $|1\rangle\langle 1|$ . Explicitly,

$$p_{Y|X}(\ell|0) = \frac{((1 - \eta)\bar{n}_B)^\ell}{(1 + (1 - \eta)\bar{n}_B)^{\ell+1}}, \quad (43)$$

then, for  $0 \leq \bar{n}_S \leq 1$ , Corollary 2 implies that the active input is  $\hat{\rho}_{A,\text{cov}} = (1 - \bar{n}_S)|0\rangle\langle 0| + \bar{n}_S|1\rangle\langle 1|$ . Therefore

$$\begin{aligned} p_{Y|X}(\ell|1) &= (1 - \bar{n}_S) \frac{((1 - \eta)\bar{n}_B)^\ell}{(1 + (1 - \eta)\bar{n}_B)^{\ell+1}} \\ &\quad + \bar{n}_S \sum_{t=0}^1 \sum_{u=0}^{\ell} (-1)^{t+u} \binom{1}{t} \binom{\ell}{u} \\ &\quad \eta^t \frac{(t+u)!}{t!u!} \frac{1}{(1 + (1 - \eta)\bar{n}_B)^{t+u+1}}. \end{aligned} \quad (44)$$

Hence the mutual information of the binary asymmetric channel is

$$\begin{aligned} I_\alpha(X; Y) &= (1 - \alpha) \sum_{\ell=0}^{\infty} p_{Y|X}(\ell|0) \log \frac{p_{Y|X}(\ell|0)}{p_\alpha(\ell)} \\ &\quad + \alpha \sum_{\ell=0}^{\infty} p_{Y|X}(\ell|1) \log \frac{p_{Y|X}(\ell|1)}{p_\alpha(\ell)}, \end{aligned} \quad (45)$$

where

$$p_\alpha(\ell) = (1 - \alpha) p_{Y|X}(\ell|0) + \alpha p_{Y|X}(\ell|1). \quad (46)$$

For fixed  $\bar{n}_S$ , as  $\alpha \rightarrow 0$ , the mutual information satisfies  $I_\alpha(X; Y) = \alpha \sum_{\ell \in \mathcal{Y}} p_{Y|X}(\ell|1) \log \frac{p_{Y|X}(\ell|1)}{p_{Y|X}(\ell|0)} + o(\alpha)$ . Under the covertness budget,  $\alpha$  is maximized when equal to  $\sqrt{\frac{2\delta}{nC_P}}$ , therefore, the covert communication capability for the covertness-optimized sparse input is

$$\begin{aligned} C_{\text{cov,opt}}(\bar{n}_S) &= \lim_{n \rightarrow \infty} \sqrt{n} I_\alpha(X; Y) \\ &= \sqrt{\frac{2\delta}{C_P}} \sum_{\ell \in \mathcal{Y}} p_{Y|X}(\ell|1) \log \frac{p_{Y|X}(\ell|1)}{p_{Y|X}(\ell|0)}. \end{aligned} \quad (47)$$

Operationally, this means that any message set satisfying  $\log |\mathcal{M}_n| \leq \sqrt{n} C_{\text{cov,opt}}(\bar{n}_S) - o(\sqrt{n})$  can be transmitted with  $P_e^{(b)} \rightarrow 0$  while satisfying the covertness constraint.

Now, for the functionality-optimized communication scheme, each active use employs circularly symmetric complex Gaussian coherent-state modulation. It is well known that this ensemble achieves the Holevo information of the bosonic channel [7], [31]. In this scheme, Alice transmits with probability  $\alpha$ , and on each active use prepares a coherent state  $|\epsilon\rangle$  whose amplitude is drawn from a circularly symmetric complex Gaussian distribution with mean photon number  $\bar{n}_S$ , i.e.,  $\epsilon \sim \mathcal{CN}(0, \bar{n}_S)$ . Equivalently, the sparse input state is

$$\hat{\rho}_{\text{sp},\epsilon} = (1 - \alpha) |0\rangle\langle 0| + \alpha \int_{\mathbb{C}} \frac{1}{\pi \bar{n}_S} e^{-|\epsilon|^2/\bar{n}_S} |\epsilon\rangle\langle \epsilon| d^2\epsilon. \quad (48)$$

The Gaussian average in (48) is the thermal state  $\hat{\rho}_{\text{th}}(\bar{n}_S)$ . Hence Willie sees a thermal active-state output in this case. The corresponding Holevo information is then,

$$\chi_{\text{Hol}}(\bar{n}_S) = g((1 - \eta)\bar{n}_B + \eta\bar{n}_S) - g((1 - \eta)\bar{n}_B), \quad (49)$$

where  $g(x) = (x + 1) \log(x + 1) - x \log x$ . After applying the same covertness scaling the covert communication capability is then

$$C_{\text{cov,G}}(\bar{n}_S) = \sqrt{\frac{2\delta}{C_G}} \chi_{\text{Hol}}(\bar{n}_S), \quad (50)$$

where  $C_G = \frac{\eta_W^2 \bar{n}_S^2}{\eta \bar{n}_B (1 + \eta \bar{n}_B) - \eta_W^2 \bar{n}_S^2}$ .

Fig. 3 exhibit noticeable crossovers. At small active  $\bar{n}_S$ , Gaussian coherent-state modulation benefits from its larger active-use Holevo information  $\chi_{\text{Hol}}(\bar{n}_S)$ , and therefore can outperform the covertness-optimized Fock-diagonal state  $\hat{\rho}_{A,\text{cov}}$ . However, this gain also produces a larger Willie-side coefficient  $C_G$ , which reduces the allowable  $\alpha$  through the factor  $\sqrt{2\delta/C_G}$ . As  $\bar{n}_S$  increases, the covertness penalty dominates, causing the dotted Gaussian curves to decrease rapidly, while the solid Fock-diagonal curves become preferable.

### B. Covert Sensing Performance

For covert sensing, the relevant functionality is Alice's target-detection exponent. Since sparse signaling activates only an  $\alpha$  fraction of the available modes, only the active modes contribute to the sensing exponent, while all modes contribute to Willie's covertness constraint through the ensemble-averaged sparse state  $\hat{\rho}_\alpha$ . The quantum Chernoff exponent between Alice's returned states under  $h = 0$  and  $h = 1$  is

$$\Phi(\bar{n}_S) = -\log \left[ \min_{0 \leq s \leq 1} \text{tr} \left( \hat{\rho}_{IR}(h=0)^s \hat{\rho}_{IR}(h=1)^{1-s} \right) \right]. \quad (51)$$

The optimal target-detection error probability satisfies the Chernoff-exponent relation [32], [33]

$$\lim_{n \rightarrow \infty} -\frac{1}{n} \log P_e^{(s)}(n) = \Phi(\bar{n}_S). \quad (52)$$

We now note the role of the reference system in the sensing comparison. Alice's input sensing state is joint a signal-reference state  $\hat{\rho}_{IS}$ . Under hypothesis  $h$ , Alice receives the

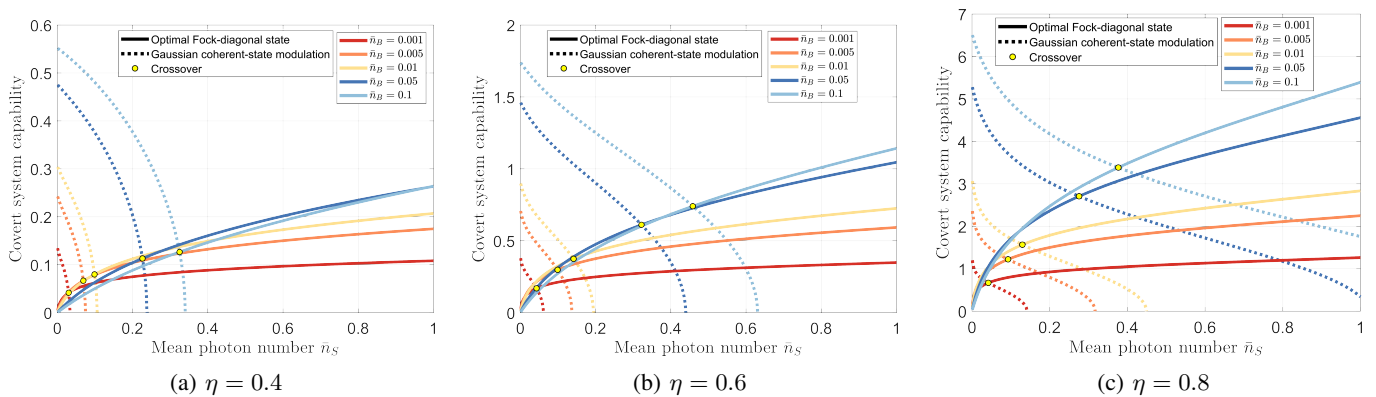


Fig. 3: Covert communication capability vs. mean photon number  $\bar{n}_S$  for sparse signaling over the thermal-loss bosonic channel. The three panels correspond to  $\eta = 0.4$ ,  $\eta = 0.6$ , and  $\eta = 0.8$ , respectively. Solid curves show the covertness-optimized Fock-diagonal input from Corollary 2; dotted curves show Gaussian coherent-state modulation, whose functionality metric is the Holevo information. Different colors correspond to different background photon numbers  $\bar{n}_B$ . Yellow markers denote the first crossover point where the covertness-optimized Fock-diagonal scheme begins to outperform Gaussian coherent-state modulation.

joint state  $\hat{\rho}_{IS}(h) = (\mathcal{I}_I \otimes \mathcal{E}^{(1-\gamma^{(h)})\tau_A, (1-\tau_A)\bar{n}_A})(\hat{\rho}_{IS})$ , The Willie-side QRE coefficient, however, depends only on the transmitted signal marginal  $\hat{\rho}_S = \text{tr}_I[\hat{\rho}_{IS}]$ , since Willie has no access to Alice's retained reference. For the covertness-optimized Fock-diagonal scheme, we use the trivial reference idler. Equivalently, one may append a fixed reference state  $\hat{\sigma}_I$  that is independent of the sensing hypothesis:  $\hat{\rho}_{IS, \text{cov}}(h) = \hat{\sigma}_I \otimes \hat{\rho}_{S, \text{cov}}(h)$ , since the same idler state  $\hat{\sigma}_I$  appears under both hypotheses, it contributes a unit factor to the Chernoff exponent. By contrast, in the sparse TMSV scheme, Alice transmits thermal signal marginal  $\hat{\rho}_{S, \text{TMSV}}$  in (39). Thus Willie observes the same transmitted signal marginal as an attenuated thermal output, while Alice retains a nontrivial idler correlated with the transmitted signal. The TMSV advantage in the sensing exponent comes from this retained idler, whereas its Willie-side covertness is determined only by the thermal signal marginal. Next, impose the maximized  $\alpha$  under covertness budget, the obtained covert sensing capability is,  $\sqrt{\frac{2\delta}{C_W}} \Phi(\bar{n}_S)$ , and consequently,  $-\log P_e^{(s)} = \sqrt{n} \sqrt{\frac{2\delta}{C_W}} \Phi(\bar{n}_S) + o(\sqrt{n})$ . Thus, the covert sensing capability is the square-root-law Chernoff coefficient: a larger value means faster decay of Alice's target-detection error probability under the same QRE covertness budget.

We now compare two sparse sensing schemes. The first uses the covertness-optimized Fock-diagonal input state from Corollary 2. Since the active state is Fock diagonal and the target-return channels are phase-insensitive, Alice's returned states under both hypothesis are diagonal in the Fock basis. Thus PNR detection reduces the target-discrimination problem to a classical hypothesis test over photon counts. The corresponding single-active-mode Chernoff exponent is

$$\Phi_{\text{cov, opt}}(\bar{n}_S) = -\log \min_{0 \leq s \leq 1} \sum_{\ell=0}^{\infty} (p_\ell(h=0))^s (p_\ell(h=1))^{1-s}, \quad (53)$$

where

$$p_\ell(h) = (1 - \bar{n}_S) p_{\ell|0}(h) + \bar{n}_S p_{\ell|1}(h) \quad (54)$$

and the conditional photon-count distribution is

$$p_{\ell|i}(h) = \sum_{t=0}^1 \sum_{u=0}^{\ell} (-1)^{t+u} \binom{i}{t} \binom{\ell}{u} \left( (1 - \gamma^{(h)})\tau_A \right)^t \frac{(t+u)!}{t!u!} \frac{1}{(1 + ((1 - \tau_A)\bar{n}_A))^{t+u+1}}. \quad (55)$$

Therefore, the covert sensing capability of the Fock-diagonal strategy is

$$\mathcal{S}_{\text{cov, opt}}(\bar{n}_S) = \sqrt{\frac{2\delta}{C_{P, \text{se}}}} \Phi_{\text{cov, opt}}(\bar{n}_S). \quad (56)$$

where  $C_{P, \text{se}} = \frac{(\tau_W \bar{n}_S)^2}{((1 - \tau_W)\bar{n}_W)(1 + ((1 - \tau_W)\bar{n}_W))}$ .

The second scheme is sparse TMSV signaling. We consider TMSV because they optimize the Chernoff exponent among Gaussian inputs, are near-optimal in the low-reflectance regime [34], and optimize the missed-detection/false-alarm tradeoff among all input states [35]. Let  $\hat{\rho}_{IR}^{\text{TMSV}}(h)$  denote Alice's signal-idler state under hypothesis  $h$ . The corresponding single-active-mode Chernoff exponent is

$$\Phi_{\text{TMSV}}(\bar{n}_S) = -\log \min_{0 \leq s \leq 1} \text{tr} \left[ (\hat{\rho}_{IR}^{\text{TMSV}}(0))^s (\hat{\rho}_{IR}^{\text{TMSV}}(1))^{1-s} \right]. \quad (57)$$

The corresponding covert sensing capability is then

$$\mathcal{S}_{\text{TMSV}}(\bar{n}_S) = \sqrt{\frac{2\delta}{C_{\text{TMSV}}}} \Phi_{\text{TMSV}}(\bar{n}_S). \quad (58)$$

where  $C_{\text{TMSV}} = \frac{(\tau_W \bar{n}_S)^2}{((1 - \tau_W)\bar{n}_W)(1 + ((1 - \tau_W)\bar{n}_W)) - (\tau_W \bar{n}_S)^2}$ ,

As shown in Fig. 4, the consistent tradeoff are: at small  $\bar{n}_S$ , the sparse TMSV can benefit from the retained idler and achieve a larger active-mode Chernoff exponent. However,

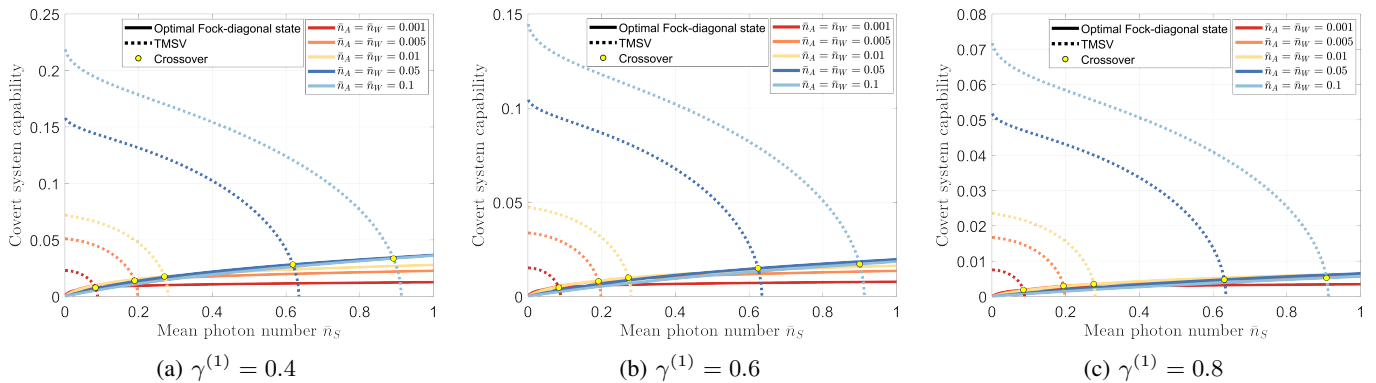


Fig. 4: Covert sensing capability vs. mean photon number  $\bar{n}_S$  for sparse signaling with  $\tau_A = \tau_W = 0.3$ . The three panels correspond to target-present parameters  $\gamma^{(1)} = 0.4$ ,  $\gamma^{(1)} = 0.6$ , and  $\gamma^{(1)} = 0.8$ , respectively. Solid curves show the covertness-optimized Fock-diagonal probe from Corollary 2; dotted curves show the sparse TMSV benchmark. Different colors correspond to different background photon numbers  $\bar{n}_B$ . Yellow markers denote the first crossover point where the covertness-optimized Fock-diagonal scheme begins to outperform sparse TMSV.

this improvement also increases Willie’s QRE coefficient, as reflected by the denominator in  $C_{\text{TMSV}}$ . As  $\bar{n}_S$  increases, the stronger covertness penalty of TMSV offsets its sensing advantage, and the covertness-optimized Fock-diagonal scheme becomes preferable. Compared with the communication case, the crossover behavior in sensing is less pronounced. The TMSV advantage is mainly confined to the low- $\bar{n}_S$  region, while the covertness-optimized Fock-diagonal state  $\hat{\rho}_{A,\text{cov}}$  remains competitive over a broad range of  $\bar{n}_S$ .

## VI. CONCLUSION

We studied sparse covert signaling over lossy thermal-noise bosonic channels. We then characterized the active input quantum state that minimizes Willie’s leading QRE coefficient under a mean photon number constraint.

The main result is that an optimal active input can be chosen diagonal in the Fock basis and supported on at most two consecutive photon numbers. In the relevant covert brightness regime the optimizer is reduced to a vacuum and single-photon mixture. We further showed that the covertness-optimized active input state saturates bosonic covert-communication converse [7] and matches the near-optimal TSMV diffuse scheme [9]. The resulting performance tradeoff shows the optimality of the minimizer state: it offers notable advantage in covert operations under moderate mean photon numbers.

We note that if the perturbative expansion in [24] was valid for infinite dimensionality, then one could use it to derive identical QRE expansion, motivating future exploration of extension of perturbation theory of quantum information.

## ACKNOWLEDGMENT

The authors acknowledge helpful discussions with Saikat Guha, Mehrdad Tahmasbi, Matthieu R. Bloch, and Uzi Pereg.

## REFERENCES

- [1] B. A. Bash, D. Goeckel, and D. Towsley, “Square root law for communication with low probability of detection on AWGN channels,” in *Proc. IEEE Int. Symp. Inform. Theory (ISIT)*, Cambridge, MA, Jul. 2012.
- [2] —, “Limits of reliable communication with low probability of detection on AWGN channels,” *IEEE J. Sel. Areas Commun.*, vol. 31, no. 9, pp. 1921–1930, Sep. 2013.
- [3] M. R. Bloch, “Covert communication over noisy channels: A resolvability perspective,” *IEEE Transactions on Information Theory*, vol. 62, no. 5, pp. 2334–2354, 2016.
- [4] L. Wang, “Optimal throughput for covert communication over a classical-quantum channel,” in *Proc. Inform. Theory Workshop (ITW)*, Cambridge, UK, Sep. 2016, pp. 364–368, arXiv:1603.05823 [cs.IT].
- [5] B. A. Bash, A. H. Gheorghie, M. Patel, J. L. Habif, D. Goeckel, D. Towsley, and S. Guha, “Quantum-secure covert communication on bosonic channels,” *Nat. Commun.*, vol. 6, Oct. 2015.
- [6] X. Chen, J. An, Z. Xiong, C. Xing, N. Zhao, F. R. Yu, and A. Nallanathan, “Covert communications: A comprehensive survey,” *IEEE Commun. Surv. Tutor.*, vol. 25, no. 2, pp. 1173–1198, 2023.
- [7] M. S. Bullock, C. N. Gagatsos, S. Guha, and B. A. Bash, “Fundamental Limits of Quantum-Secure Covert Communication Over Bosonic Channels,” *IEEE Journal on Selected Areas in Communications*, vol. 38, no. 3, pp. 471–482, Mar. 2020.
- [8] C. N. Gagatsos, M. S. Bullock, and B. A. Bash, “Covert capacity of bosonic channels,” *IEEE J. Sel. Areas Inf. Theory*, vol. 1, pp. 555–567, 2020.
- [9] M. Tahmasbi, B. A. Bash, S. Guha, and M. Bloch, “Signaling for covert quantum sensing,” in *Proc. IEEE Int. Symp. Inform. Theory (ISIT)*, 2021, pp. 1041–1045.
- [10] R. Bali, T. E. Bailey, M. S. Bullock, and B. A. Bash, “Experimental validation of provably covert communication using software-defined radio,” *IEEE Journal on Selected Areas in Communications*, 2026.
- [11] C. Weedbrook, S. Pirandola, R. García-Patrón, N. J. Cerf, T. C. Ralph, J. H. Shapiro, and S. Lloyd, “Gaussian quantum information,” *Rev. Mod. Phys.*, vol. 84, pp. 621–669, May 2012.
- [12] M. O. Scully and M. S. Zubairy, *Quantum Optics*. Cambridge, UK: Cambridge University Press, 1997.
- [13] D. F. Walls and G. J. Milburn, *Quantum Optics*. Springer, 2008.
- [14] G. S. Agarwal, *Quantum Optics*. Cambridge, UK: Cambridge University Press, 2012.
- [15] M. Orszag, *Quantum Optics*, 3rd ed. Berlin, Germany: Springer, 2016.
- [16] M. S. Bullock, C. N. Gagatsos, S. Guha, and B. A. Bash, “Fundamental limits of quantum-secure covert communication over bosonic channels,” *IEEE J. Sel. Areas Commun.*, vol. 38, no. 3, pp. 471–482, Mar. 2020.
- [17] E. J. D. Anderson, C. K. Eyre, I. M. Dailey, F. Rozpędek, and B. A. Bash, “Square root law for covert quantum communication over optical channels,” in *Proc. IEEE Int. Conf. Quantum Comput. Eng. (QCE)*, Montréal, QC, Canada, 2024.
- [18] E. J. D. Anderson, M. S. Bullock, F. Rozpędek, and B. A. Bash, “Achievability of covert quantum communication,” in *IEEE Int. Symp. Inf. Theory (ISIT)*, 2025.
- [19] S.-H. Tan, B. I. Erkmen, V. Giovannetti, S. Guha, S. Lloyd, L. Maccone, S. Pirandola, and J. H. Shapiro, “Quantum illumination with gaussian states,” *Phys. Rev. Lett.*, vol. 101, p. 253601, Dec. 2008.

- [20] C. W. Helstrom, *Quantum Detection and Estimation Theory*. New York, NY, USA: Academic Press, Inc., 1976.
- [21] M. Wilde, *Quantum Information Theory*, 2nd ed. Cambridge University Press, 2016.
- [22] C. N. Gagatsos, M. S. Bullock, and B. A. Bash, "Covert capacity of bosonic channels," Accepted for publication by IEEE J. Sel. Areas Inf. Theory, arXiv:2002.06733 [quant-ph], 2020.
- [23] E. J. D. Anderson, M. S. Bullock, F. Rzepdek, and B. A. Bash, "Achievability of covert quantum communication," 2025, presented at the 2025 IEEE Int. Symp. Inf. Theory (ISIT).
- [24] M. R. Grace and S. Guha, "Perturbation theory for quantum information," in *2022 IEEE Information Theory Workshop (ITW)*. IEEE, 2022, pp. 500–505.
- [25] C. Weedbrook, S. Pirandola, R. García-Patrón, N. J. Cerf, T. C. Ralph, J. H. Shapiro, and S. Lloyd, "Gaussian quantum information," *Reviews of modern physics*, vol. 84, no. 2, pp. 621–669, 2012.
- [26] S. D. Bartlett, T. Rudolph, and R. W. Spekkens, "Reference frames, superselection rules, and quantum information," *Reviews of Modern Physics*, vol. 79, no. 2, pp. 555–609, 2007.
- [27] R. Koekoek and R. F. Swarttouw, "The askey-scheme of hypergeometric orthogonal polynomials and its q-analogue," *arXiv preprint math/9602214*, 1996.
- [28] C. Niculescu and L.-E. Persson, *Convex functions and their applications*. Springer, 2006, vol. 23.
- [29] S. Pirandola, "Limits and security of free-space quantum communications," *Physical Review Research*, vol. 3, no. 1, p. 013279, 2021.
- [30] M. Ghalaii and S. Pirandola, "Quantum communications in a moderate-to-strong turbulent space," *Communications Physics*, vol. 5, no. 1, p. 38, 2022.
- [31] C. Lupo, S. Pirandola, P. Aniello, and S. Mancini, "On the classical capacity of quantum gaussian channels," *Physica Scripta*, vol. 2011, no. T143, p. 014016, 2011.
- [32] K. M. R. Audenaert, J. Calsamiglia, R. Muñoz Tapia, E. Bagan, L. Masanes, A. Acin, and F. Verstraete, "Discriminating states: The quantum chernoff bound," *Phys. Rev. Lett.*, vol. 98, p. 160501, Apr. 2007.
- [33] M. Nussbaum and A. Szkoła, "The chernoff lower bound for symmetric quantum hypothesis testing," *Ann. Statist.*, vol. 37, no. 2, pp. 1040–1057, Apr. 2009.
- [34] M. Bradshaw, L. O. Conlon, S. Tserkis, M. Gu, P. K. Lam, and S. M. Assad, "Optimal probes for continuous-variable quantum illumination," *Physical Review A*, vol. 103, no. 6, p. 062413, 2021.
- [35] G. De Palma and J. Borregaard, "Minimum error probability of quantum illumination," *Phys. Rev. A*, vol. 98, p. 012101, Jul. 2018.
- [36] J. H. Shapiro, "The quantum theory of optical communications," *IEEE journal of selected topics in Quantum Electronics*, vol. 15, no. 6, pp. 1547–1569, 2009.

## APPENDIX I

*Proof: Lemma 1:* Let  $\hat{a}$  and  $\hat{e}$  be annihilation operators of the input and environment modes, respectively. Under the beam-splitter relation [36] of the thermal-loss channel, Willie's output mode is

$$\hat{w} = \sqrt{1-\eta}\hat{a} - \sqrt{\eta}\hat{e}. \quad (59)$$

Hence the anti-normally ordered characteristic function of Willie's output factors as

$$\chi_{\hat{\rho}_W}(\zeta) = \chi_{\hat{\rho}_A}(\sqrt{1-\eta}\zeta) \chi_{\hat{\rho}_E}(-\sqrt{\eta}\zeta). \quad (60)$$

Since the environment is thermal with mean photon number  $\bar{n}_B$ ,

$$\chi_{\hat{\rho}_E}(-\sqrt{\eta}\zeta) = \exp(-(1+\bar{n}_B)\eta|\zeta|^2). \quad (61)$$

For the Fock-diagonal input state  $\hat{\rho}_A = \sum_{i=0}^j \rho_i |i\rangle\langle i|$ ,

$$\begin{aligned} \chi_{\hat{\rho}_A}(\xi) &= \exp(-(1-\eta)|\zeta|^2) \text{tr}[\hat{\rho}_A \exp(\xi \hat{a}^\dagger) \exp(-\xi^* \hat{a})] \\ &= e^{-(1-\eta)|\zeta|^2} \sum_{i=0}^j \rho_i \langle i | e^{\xi \hat{a}^\dagger} e^{-\xi^* \hat{a}} | i \rangle, \end{aligned} \quad (62)$$

with  $\xi = \sqrt{1-\eta}\zeta$ .

Now, expanding the exponentials,

$$\langle i | \exp(\xi \hat{a}^\dagger) \exp(-\xi^* \hat{a}) | i \rangle = \sum_{t=0}^{\infty} \sum_{u=0}^{\infty} \frac{\xi^t (-\xi^*)^u}{t! u!} \langle i | (\hat{a}^\dagger)^t \hat{a}^u | i \rangle. \quad (63)$$

Using orthogonality, only terms with equal numbers of annihilation and creation operators survive; i.e, when  $t = u = s$ . Thus

$$\langle i | \exp(\xi \hat{a}^\dagger) \exp(-\xi^* \hat{a}) | i \rangle = \sum_{s=0}^i \frac{\xi^s (-\xi^*)^s}{(s!)^2} \langle i | (\hat{a}^\dagger)^s \hat{a}^s | i \rangle. \quad (64)$$

Using  $\hat{a}^s | i \rangle = \sqrt{\frac{i!}{(i-s)!}} | i-s \rangle$  and then applying  $(\hat{a}^\dagger)^s$  back yields

$$\langle i | (\hat{a}^\dagger)^s \hat{a}^s | i \rangle = \frac{i!}{(i-s)!}. \quad (65)$$

Therefore,

$$\begin{aligned} \langle i | \exp(\xi \hat{a}^\dagger) \exp(-\xi^* \hat{a}) | i \rangle &= \sum_{s=0}^i \frac{i!}{(i-s)!} \frac{(-|\xi|^2)^s}{(s!)^2} \\ &= \sum_{s=0}^i \binom{i}{s} \frac{(-|\xi|^2)^s}{s!} \\ &= L_i(|\xi|^2) = L_i((1-\eta)|\zeta|^2). \end{aligned} \quad (66)$$

Substitute (66) into (62) to get Willie's output characteristic function:

$$\chi_{\hat{\rho}_W}(\zeta) = e^{-(1+\eta\bar{n}_B)|\zeta|^2} \sum_{i=0}^j \rho_i L_i((1-\eta)|\zeta|^2). \quad (67)$$

Now reconstruct the state  $\hat{\rho}_W$  by Fourier inversion:

$$\hat{\rho}_W = \int_{\mathbb{C}} \pi^{-1} d^2\zeta \chi_{\hat{\rho}_W}(\zeta) e^{\zeta \hat{w}^\dagger} e^{-\zeta^* \hat{w}}. \quad (68)$$

Taking Fock matrix elements  $\langle \ell | \hat{\rho}_W | \ell' \rangle$ , writing  $\zeta = r e^{i\theta}$ , and using that (67) depends only on  $r^2 = |\zeta|^2$ , the angular integration yields:

$$\int_0^{2\pi} \langle \ell | e^{r e^{i\theta} \hat{w}^\dagger} e^{-r e^{-i\theta} \hat{w}} | \ell' \rangle d\theta = 2\pi L_\ell(r^2) \delta_{\ell, \ell'}. \quad (69)$$

Thus  $\langle \ell | \hat{\rho}_W | \ell' \rangle = 0$  for  $\ell \neq \ell'$ , so  $\hat{\rho}_W$  is diagonal,  $p_\ell = \langle \ell | \hat{\rho}_W | \ell \rangle$ , then

$$p_\ell = 2 \int_0^\infty r dr \chi_{\hat{\rho}_W}(r) L_\ell(r^2). \quad (70)$$

Setting  $x = r^2$ , so that  $dx = 2r dr$ , then gives (20). Finally, expanding both Laguerre polynomials in (20) according to the Laguerre polynomials series expansion and integrating term-by-term with  $\int_0^\infty x^s e^{-ax} dx = s!/a^{s+1}$ ,  $a = 1 + \eta\bar{n}_b$ , yields (21). This completes the proof. ■

## APPENDIX II

*Proof: Lemma 2:*

Willie's innocent thermal state is,

$$\hat{\rho}_{\text{th}}(\eta\bar{n}_{\text{B}}) = \sum_{\ell=0}^{\infty} \lambda_{\ell} |\ell\rangle\langle\ell|, \quad (71)$$

where

$$\lambda_{\ell} = \frac{(\eta\bar{n}_{\text{B}})^{\ell}}{(1 + \eta\bar{n}_{\text{B}})^{\ell+1}}, \quad \sum_{\ell=0}^{\infty} \lambda_{\ell} = 1, \quad (72)$$

and Willie's non-innocent output state is,

$$\hat{\rho}_W = \sum_{\ell=0}^{\infty} p_{\ell} |\ell\rangle\langle\ell|, \quad (73)$$

where  $p_{\ell}$  is expressed as(20).

For convenience, define,

$$\hat{\rho}_{\alpha} = \sum_{\ell=0}^{\infty} p_{\alpha,\ell} |\ell\rangle\langle\ell|, \quad (74)$$

where,

$$p_{\alpha,\ell} = (1 - \alpha)\lambda_{\ell} + \alpha p_{\ell} = \lambda_{\ell} + \alpha(p_{\ell} - \lambda_{\ell}). \quad (75)$$

Also, define,

$$h_{\ell} = p_{\ell} - \lambda_{\ell}, \quad r_{\ell} = \frac{h_{\ell}}{\lambda_{\ell}}. \quad (76)$$

Then

$$p_{\alpha,\ell} = \lambda_{\ell}(1 + \alpha r_{\ell}). \quad (77)$$

Since both  $\{\lambda_{\ell}\}$  and  $\{p_{\ell}\}$  are probability distributions,

$$\sum_{\ell=0}^{\infty} h_{\ell} = \sum_{\ell=0}^{\infty} p_{\ell} - \sum_{\ell=0}^{\infty} \lambda_{\ell} = 0. \quad (78)$$

Equivalently,

$$\sum_{\ell=0}^{\infty} \lambda_{\ell} r_{\ell} = 0. \quad (79)$$

Now, since Willie's innocent thermal state and non-innocent output state are both diagonal in the Fock-basis. Therefore, the QRE in (15) reduced to a classical KL divergence,

$$D(\hat{\rho}_{\alpha} \parallel \hat{\rho}_{\text{th}}(\eta\bar{n}_{\text{B}})) = \sum_{\ell=0}^{\infty} p_{\alpha,\ell} \log \frac{p_{\alpha,\ell}}{\lambda_{\ell}} \quad (80)$$

$$= \sum_{\ell=0}^{\infty} \lambda_{\ell} (1 + \alpha r_{\ell}) \log(1 + \alpha r_{\ell}). \quad (81)$$

Using (79), we subtract the vanishing first-order term:

$$D(\hat{\rho}_{\alpha} \parallel \hat{\rho}_{\text{th}}(\eta\bar{n}_{\text{B}})) = \sum_{\ell=0}^{\infty} \lambda_{\ell} [(1 + \alpha r_{\ell}) \log(1 + \alpha r_{\ell}) - \alpha r_{\ell}]. \quad (82)$$

let

$$g(x) = (1 + x) \log(1 + x) - x. \quad (83)$$

Then

$$g(0) = 0, \quad g'(0) = 0, \quad g''(x) = \frac{1}{1+x}. \quad (84)$$

Therefore, for each fixed  $\ell$ ,

$$\left. \frac{d^2}{d\alpha^2} \lambda_{\ell} g(\alpha r_{\ell}) \right|_{\alpha=0} = \lambda_{\ell} r_{\ell}^2. \quad (85)$$

Since

$$\lambda_{\ell} r_{\ell}^2 = \frac{(p_{\ell} - \lambda_{\ell})^2}{\lambda_{\ell}}, \quad (86)$$

the formal second derivative is

$$\left. \frac{d^2}{d\alpha^2} D(\hat{\rho}_{\alpha} \parallel \hat{\rho}_{\text{th}}(\eta\bar{n}_{\text{B}})) \right|_{\alpha=0} = \sum_{\ell=0}^{\infty} \frac{(p_{\ell} - \lambda_{\ell})^2}{\lambda_{\ell}}. \quad (87)$$

Assume the finite-coefficient condition

$$C_P = \sum_{\ell=0}^{\infty} \frac{(p_{\ell} - \lambda_{\ell})^2}{\lambda_{\ell}} < \infty. \quad (88)$$

Then the term-by-term differentiation is justified by dominated convergence. Indeed, fix  $0 < \alpha_0 < 1$ . For  $0 \leq \alpha \leq \alpha_0$ , since  $p_{\ell} \geq 0$ , we have

$$r_{\ell} = \frac{p_{\ell} - \lambda_{\ell}}{\lambda_{\ell}} \geq -1. \quad (89)$$

Hence  $1 + \alpha r_{\ell} \geq 1 - \alpha_0$  when  $r_{\ell} < 0$ , while  $1 + \alpha r_{\ell} \geq 1$  when  $r_{\ell} \geq 0$ . Therefore,

$$0 \leq \frac{\lambda_{\ell} r_{\ell}^2}{1 + \alpha r_{\ell}} \leq \frac{\lambda_{\ell} r_{\ell}^2}{1 - \alpha_0}. \quad (90)$$

The right-hand side is summable because

$$\sum_{\ell=0}^{\infty} \lambda_{\ell} r_{\ell}^2 = C_P < \infty. \quad (91)$$

Thus one may differentiate the infinite sum twice at  $\alpha = 0$ , giving

$$f''(0) = C_P, \quad f(\alpha) = D(\hat{\rho}_{\alpha} \parallel \hat{\rho}_{\text{th}}(\eta\bar{n}_{\text{B}})). \quad (92)$$

Finally,  $f(0) = 0$  and  $f'(0) = 0$ . Therefore the Taylor expansion gives

$$D(\hat{\rho}_{\alpha} \parallel \hat{\rho}_{\text{th}}(\eta\bar{n}_{\text{B}})) = \frac{\alpha^2}{2} C_P + o(\alpha^2), \quad (93)$$

that is,

$$D(\hat{\rho}_{\alpha} \parallel \hat{\rho}_{\text{th}}(\eta\bar{n}_{\text{B}})) = \frac{\alpha^2}{2} \sum_{\ell=0}^{\infty} \frac{(p_{\ell} - \lambda_{\ell})^2}{\lambda_{\ell}} + o(\alpha^2). \quad (94)$$

■

## APPENDIX III

*Proof: Lemma 3:* We work under the assumptions of lemma 1, lemma 2, and use Definition III.4. Thus the input is Fock-diagonal,

$$\hat{\rho}_A = \sum_{i=0}^j \rho_i |i\rangle \langle i|, \quad \rho_i \geq 0, \quad \sum_{i=0}^j \rho_i = 1, \quad (95)$$

and Willie's active output is diagonal,

$$\hat{\rho}_W = \sum_{\ell=0}^{\infty} p_\ell |\ell\rangle \langle \ell|. \quad (96)$$

By lemma 2,

$$C_P = \sum_{\ell=0}^{\infty} \frac{(p_\ell - \lambda_\ell)^2}{\lambda_\ell}, \quad (97)$$

where

$$\lambda_\ell = \frac{(\eta \bar{n}_B)^\ell}{(1 + \eta \bar{n}_B)^{\ell+1}}. \quad (98)$$

From Lemma 1, the output transition probabilities admit the integral representation

$$\mathcal{I}_{\ell,i} = \int_0^\infty e^{-(1+\eta \bar{n}_B)x} L_\ell(x) L_i((1-\eta)x) dx, \quad (99)$$

so that

$$p_\ell = \sum_{i=0}^m \rho_i \mathcal{I}_{\ell,i}, \quad \lambda_\ell = \mathcal{I}_{\ell,0}. \quad (100)$$

Using  $\sum_{i=0}^j \rho_i = 1$ , we may rewrite

$$p_\ell - \lambda_\ell = \sum_{i=1}^m \rho_i (\mathcal{I}_{\ell,i} - \mathcal{I}_{\ell,0}). \quad (101)$$

Substituting (101) into (97) gives

$$C_P = \sum_{\ell=0}^{\infty} \frac{1}{\lambda_\ell} \left( \sum_{i=1}^j \rho_i (\mathcal{I}_{\ell,i} - \mathcal{I}_{\ell,0}) \right)^2. \quad (102)$$

We next normalize by the innocent distribution. Define

$$R_i(\ell) = \frac{\mathcal{I}_{\ell,i}}{\lambda_\ell}, \quad S(\ell) = \frac{p_\ell}{\lambda_\ell} = \sum_{i=0}^j \rho_i R_i(\ell). \quad (103)$$

Then (97) becomes

$$C_P = \sum_{\ell=0}^{\infty} \lambda_\ell (S(\ell) - 1)^2. \quad (104)$$

We now identify the orthogonal basis adapted to  $\lambda_\ell$ . Let

$$q = \frac{\eta \bar{n}_B}{1 + \eta \bar{n}_B}, \quad \theta = \frac{1 - \eta}{1 + \eta \bar{n}_B}. \quad (105)$$

Since

$$\lambda_\ell = \frac{(\eta \bar{n}_B)^\ell}{(1 + \eta \bar{n}_B)^{\ell+1}} = (1 - q)q^\ell, \quad (106)$$

the sequence  $\{\lambda_\ell\}_{\ell \geq 0}$  is geometric. We therefore use the Meixner polynomials  $M_y(\ell; q)$ , whose generating function is

$$\sum_{y=0}^{\infty} M_y(\ell; q) \nu^y = \left(1 - \frac{\nu}{q}\right)^\ell (1 - \nu)^{-\ell-1}, \quad |\nu| < 1, \quad (107)$$

and whose orthogonality relation under  $\lambda_\ell$  is

$$\sum_{\ell=0}^{\infty} \lambda_\ell M_y(\ell; q) M_{y'}(\ell; q) = q^{-y} \delta_{y,y'}. \quad (108)$$

To expand  $R_i(\ell)$  in this basis, consider the generating function

$$G_\ell(s) = \sum_{i=0}^{\infty} \mathcal{I}_{\ell,i} s^i. \quad (109)$$

Using the Laguerre polynomial generating function

$$\sum_{i=0}^{\infty} L_i((1-\eta)x) s^i = \frac{1}{1-s} \exp\left(-\frac{(1-\eta)xs}{1-s}\right), \quad (110)$$

together with (99), we obtain

$$G_\ell(s) = \frac{1}{1-s} \int_0^\infty \exp\left(-\left[1 + \eta \bar{n}_B + \frac{(1-\eta)s}{1-s}\right]x\right) L_\ell(x) dx. \quad (111)$$

Applying the Laplace-transform identity for Laguerre polynomials,

$$\int_0^\infty e^{-ax} L_\ell(x) dx = \frac{(a-1)^\ell}{a^{\ell+1}}, \quad a > 1, \quad (112)$$

yields

$$\sum_{i=0}^{\infty} R_i(\ell) s^i = \frac{G_\ell(s)}{\lambda_\ell} = (1 + (\theta/q - 1)s)^\ell (1 + (\theta - 1)s)^{-\ell-1}. \quad (113)$$

On the other hand, using (107) with  $\nu = -\frac{\theta s}{1-s}$ , together with the binomial-series identity

$$\sum_{i=y}^{\infty} \binom{i}{y} s^i = \frac{s^y}{(1-s)^{y+1}}, \quad y = 0, 1, 2, \dots, \quad (114)$$

one checks that

$$\begin{aligned} & \sum_{i=0}^{\infty} \left( \sum_{y=0}^i \binom{i}{y} (-\theta)^y M_y(\ell; q) \right) s^i \\ &= (1 + (\theta/q - 1)s)^\ell (1 + (\theta - 1)s)^{-\ell-1}. \end{aligned} \quad (115)$$

Comparing (113) and (115) shows that, for every  $i \geq 0$ ,

$$R_i(\ell) = \sum_{y=0}^i \binom{i}{y} (-\theta)^y M_y(\ell; q). \quad (116)$$

Since  $R_0(\ell) = 1$ , it follows from (103) and (116) that

$$\begin{aligned} S(\ell) - 1 &= \sum_{i=1}^j \rho_i (R_i(\ell) - 1) \\ &= \sum_{i=1}^j \rho_i \sum_{y=1}^i \binom{i}{y} (-\theta)^y M_y(\ell; q) \end{aligned}$$

$$= \sum_{y=1}^j \left[ (-\theta)^y \sum_{i=y}^j \rho_i \binom{i}{y} \right] M_y(\ell; q). \quad (117)$$

Define

$$\mu_y = \sum_{i=y}^j \rho_i \binom{i}{y}, \quad y = 1, 2, \dots, j. \quad (118)$$

Then (117) becomes

$$S(\ell) - 1 = \sum_{y=1}^j b_y M_y(\ell; q), \quad b_y = (-\theta)^y \mu_y. \quad (119)$$

Finally, substituting (119) into (104) gives

$$\begin{aligned} C_P &= \sum_{\ell=0}^{\infty} \lambda_{\ell} \left( \sum_{y=1}^j b_y M_y(\ell; q) \right)^2 \\ &= \sum_{y=1}^j \sum_{y'=1}^j b_y b_{y'} \sum_{\ell=0}^{\infty} \lambda_{\ell} M_y(\ell; q) M_{y'}(\ell; q). \end{aligned} \quad (120)$$

Applying the orthogonality relation (108), all cross terms vanish and we obtain

$$C = \sum_{y=1}^j q^{-y} b_y^2 = \sum_{y=1}^j q^{-y} \theta^{2y} \mu_y^2, \quad \mu_y = \sum_{i=y}^j \rho_i \binom{i}{y}. \quad (121)$$

which is precisely the claimed orthogonal representation. This completes the proof. ■

#### APPENDIX IV

*Proof: Lemma 4:* Let  $\mathbb{E}[I] = \kappa + \beta$ , where  $\kappa = \lfloor \mathbb{E}[I] \rfloor$  and  $\beta \in [0, 1)$ . Define

$$g = \varphi(\tau + 1) - \varphi(\tau). \quad (122)$$

Since  $\varphi$  is discrete convex, the increments  $\varphi(i+1) - \varphi(i)$  are nondecreasing in  $i$ . We claim that

$$\varphi(i) \geq \varphi(\kappa) + g(i - \kappa), \quad i \in \mathbb{Z}_{\geq 0}. \quad (123)$$

For  $i \geq \kappa$ ,

$$\varphi(i) - \varphi(\kappa) = \sum_{\kappa'=\kappa}^{i-1} (\varphi(\kappa'+1) - \varphi(\kappa')) \geq \sum_{\kappa'=\kappa}^{i-1} g = g(i - \kappa), \quad (124)$$

because each increment in the sum is at least  $g$ .

For  $i \leq \kappa$ ,

$$\varphi(\kappa) - \varphi(i) = \sum_{\kappa'=i}^{\kappa-1} (\varphi(\kappa'+1) - \varphi(\kappa')) \leq \sum_{\kappa'=i}^{\kappa-1} g = g(\kappa - i), \quad (125)$$

because each increment in the sum is at most  $g$ . Rearranging again gives (123). Thus (123) holds for all  $i \geq 0$ .

Taking expectation with respect to  $I$  yields

$$\begin{aligned} \mathbb{E}[\varphi(I)] &\geq \mathbb{E}[\varphi(\kappa) + g(I - \kappa)] = \varphi(\kappa) + g(\mathbb{E}[I] - \kappa) \\ &= \varphi(\kappa) + g\beta. \end{aligned} \quad (126)$$

Substituting  $g = \varphi(\kappa + 1) - \varphi(\kappa)$ , we obtain

$$\mathbb{E}[\varphi(I)] \geq (1 - \beta)\varphi(\kappa) + \beta\varphi(\kappa + 1), \quad (127)$$

which proves (31).

Finally, if  $\Pr[I = \kappa] = 1 - \beta$  and  $\Pr[I = \kappa + 1] = \beta$ , then  $\mathbb{E}[I] = \kappa + \beta$  and

$$\mathbb{E}[\varphi(I)] = (1 - \beta)\varphi(\kappa) + \beta\varphi(\kappa + 1), \quad (128)$$

so equality holds. This completes the proof. ■